CHALMERS

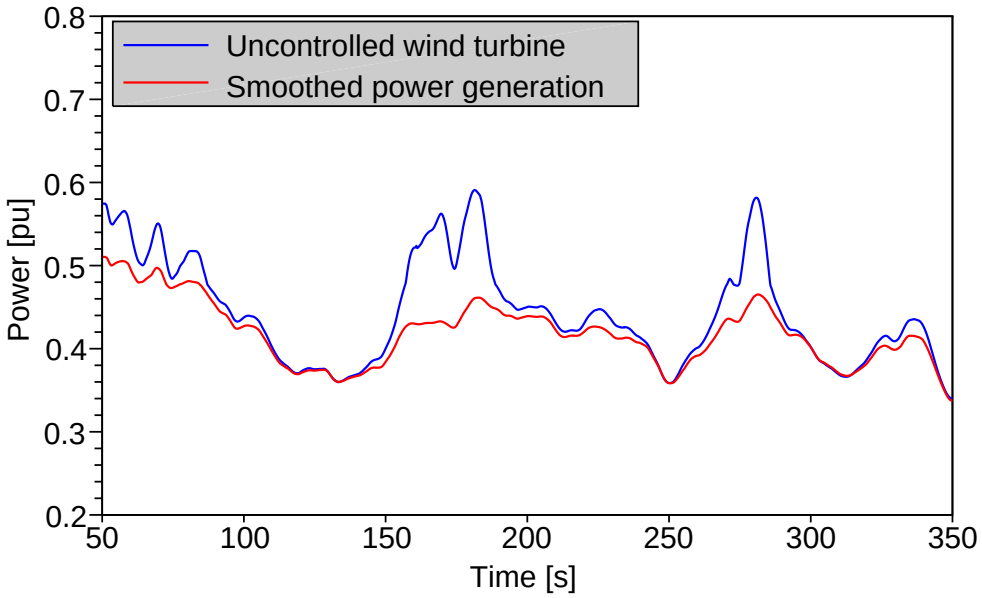

A New Wind Turbine Control Method to Smooth Power Generation

Modelling and Comparison to Wind Turbine Frequency Control

Master of Science Thesis

OLOV SOLBERG

Department of Energy and Environment
Division of Electric Power Engineering
CHALMERS UNIVERSITY OF TECHNOLOGY
Göteborg, Sweden 2012

A New Wind Turbine Control Method to Smooth Power Generation

Modelling and Comparison to Wind Turbine Frequency Control

OLOV SOLBERG

Department of Energy and Environment
Division of Electric Power Engineering
CHALMERS UNIVERSITY OF TECHNOLOGY
Göteborg, Sweden 2012

A New Wind Turbine Control Method to Smooth Power Generation
Modelling and Comparison to Wind Turbine Frequency Control
OLOV SOLBERG

Department of Energy and Environment
Division of Electric Power Engineering
CHALMERS UNIVERSITY OF TECHNOLOGY
SE–412 96 Göteborg
Sweden
Telephone +46 (0)31–772 1000

Cover:
Smoothed wind power production using a pitch angle offset of 3.3° under normal wind conditions.

Chalmers Bibliotek, Reproservice
Göteborg, Sweden 2012

A New Wind Turbine Control Method to Smooth Power Generation
Modelling and Comparison to Wind Turbine Frequency Control

OLOV SOLBERG
Department of Energy and Environment
Division of Electric Power Engineering
Chalmers University of Technology

Abstract

Following the significant increase of world wide installed wind power during the first decade of the 21st century, transmission system operators are faced with new challenges originating from the intermittent character of renewable energy sources and their installation on low and medium voltage levels. One challenge arising from the fluctuating nature of wind is to maintain frequency stability. This thesis presents a new approach to smooth the power generation of wind turbines subjected to varying wind. An active power feedback control has been developed which feeds back the momentary power generation to the turbine pitch and speed control systems. This power feedback control has been implemented in the simulation software SIMPOW and the results have been compared to a frequency control regulator for wind turbines. The frequency control was developed by the Power System Analysis Group at ÅF Industry as a part of the Swedish research initiative Elforsk.

Simulation results show that the power feedback control clearly levels the active power production of wind turbines under varying wind and thereby diminishes network frequency excursions. To achieve this, turbine deloading through a pitch angle offset is found to be imperative. The effect of different deloading levels of a turbine are evaluated, clearly demonstrating the correlation between larger deloading, enhanced frequency stability and declining energy yield. Up to wind power shares of approximately 25 %, the performance of the power feedback control is on a par with the frequency control, i.e., frequency excursions are equally subdued. Above this level of installed wind power, the frequency control is superior. Usage of the wind turbine power feedback control is discouraged because of its poorer performance, its unintuitive function and the difficulty to predict its behaviour. Lastly, the frequency control is applied to a much simplified black start case, showing the expediency of the control method to improve frequency stability, but also the extended requirement on a large turbine deloading when there are no synchronously generating units in the network.

Index Terms: Wind power, active power feedback control, frequency control, power smoothing, wind turbine deloading, fluctuating wind, black start.

Acknowledgements

This thesis was carried out at ÅF Industry, Göteborg, as a graduation from Chalmers University of Technology.

I would like to thank my examiner Peiyuan Chen at Chalmers, my supervisor Robert Josefsson at ÅF, and Mats Wang-Hansen and Haris Mehmedovic at ÅF. Thank you for your guidance and patience with my many questions, without which this work would not have been completed.

My special gratitude goes to my wife Elin. Thank you dear for always loving and supporting me.

All glory to the only wise God, through Jesus Christ, forever.

Olov Solberg
Göteborg, Sweden, 2012

Contents

List of Figures

Chapter 1

Introduction

The main objective for this master thesis project is to implement a wind turbine regulator in order to control the generation of active power. This regulator should use the active power generation as a feedback signal. The aim is to smooth wind induced frequency variations by smoothing the active power generation. To evaluate the effectiveness of the power control, a comparison to wind turbine frequency control is made. Additionally, the possibility of applying frequency control to wind turbines in black start scenarios is briefly introduced.

1.1 Background

Traditionally, electric power has been generated by large power stations such as nuclear, hydro or thermal power plants. During the entire 20^{th} century, wind power constituted an insignificant part of the total power production, making it easy for grid utilities to integrate with conventional generating facilities. From year 2001 to 2010, the amount of installed wind power worldwide has multiplied more than eight times [22]. This development has not left the electric grid industry unaffected and system operators are challenged with new stability issues. To aid in the frequency control of a power system, it is therefore advantageous if wind farms can contribute to frequency regulation. In fact, according to the draft of the upcoming harmonized European grid codes [8], all kinds of power plants will be required to assist in frequency control. However, wind power not only causes new challenges. One advantage arising with more installed wind power is the prospect of using wind turbines to black start a grid or to supply grid islands. Such a development could help reduce the number of backup diesel generators, as well as increasing power system reliability.

1.2 Purpose

The present thesis is in many ways a direct continuation of the reports [20] and [21]. These projects have been carried out by the Power System Analysis Group at ÅF Industry in Gothenburg, Sweden. The later report from ÅF, [20], presents a way to regulate the power of a wind turbine using the grid frequency deviation as an input signal. Drawing on the simulation models of that work, the purpose of this thesis project is to develop and evaluate a method to level the wind turbine power generation when using the momentary active power production as a feedback signal instead of the frequency deviation. A smooth power output will, as long as the load is constant, contribute to a smoother frequency during wind fluctuations.

One of the main goals is the comparison with the work done by ÅF, to investigate if this alternative control approach may be a viable choice. There are also many other scientific publications

dealing with the issue of frequency control support from wind power plants. Some of these articles are presented and referenced in Section 2.3, Operation of Wind Turbines.

1.3 Area of Investigation

Using the power system simulation software SIMPOW [17], the result of the above described active power control strategy is studied. First and foremost, the wind turbine active power output, rotational speed, pitch angle and grid frequency are compared. The special interest of this thesis lies in the implementation and evaluation of the power control method when using the active power as a feedback signal to the turbine speed and pitch controllers. Further, this work incorporates experimental wind data which subjects the simulated wind turbine to fluctuating, i.e., realistic, wind conditions.

1.4 Outline of Report

Following the introduction in Chapter 1, Chapter 2 first presents an overview of the theory of power system frequency control. After that, different wind turbine systems are explained as well as different operational strategies and ways to deload a wind turbine. The 3rd chapter is dedicated to a description of the default wind turbine model used in SIMPOW. Chapter 4 details the different control strategies used in this work and Chapter 5 describes the improvements done to the default SIMPOW wind power model. The simulation set up and results are presented and analysed in Chapter 6. As an extension to the initial frequency control problem, an application of wind turbines to power system black start is thereafter presented in Chapter 7. Finally, conclusions are presented in Chapter 8 together with an outlook of future work.

Chapter 2

Frequency Control of Power Systems with Wind Power

In electric power systems, many power plants cooperate to make sure that the electric load is supplied. Synchronous generators form the bulk of this generation capacity, especially in steam and hydro power plants. To secure a safe power system operation, there has to be control systems for active and reactive power, influencing mainly the grid frequency and voltage. Apart from conventional generation, modern power systems include a larger share of renewable generation such as wind and solar power. To make these integrate well with the rest of the power system, different operational strategies are continuously being developed, especially for wind turbines. There are also different wind turbine-generator configurations, providing different control possibilities. The following chapter provides a condensed theoretical overview of these topics, which have been deemed relevant to this report.

2.1 Power System Frequency Control Principles

Maintaining the power system frequency is a matter of maintaining the balance between power production and consumption. Since the use of large scale power storage systems is very limited today, the electric power production has to match the electric power consumption at any given moment. If it does, there is an active power balance in the system and the frequency will remain constant. If it does not, the frequency will change. In large interconnected systems, frequency variations seldom exceed ± 0.1 Hz [7], whereas in autonomous island systems, frequency variations up to ± 1 Hz are not uncommon [4].

In today's power system, mainly synchronous generators are used to produce electric power. These generators induce voltages with the same frequency as the rotational speed of the unit, except for the scaling of the number of pole pairs. This means that when the grid frequency changes, it does so because the speed of the synchronous generators are changing. Looking at each generator, to maintain steady state there has to be a balance between the driving mechanical torque T_m and the braking electrical torque T_e. This relation can be expressed as

$$T_m - T_e = J\frac{d\omega}{dt} \tag{2.1}$$

where J is the moment of inertia of the system and ω is the generator speed. The moment of inertia is the sum of the turbine, shaft and rotor inertia. Since torque is equal to power divided by angular frequency, $\frac{d\omega}{dt}$ will equal zero if the mechanically supplied power P_m equals the electrically generated power P_e, neglecting generator losses. From (2.1) it can also be seen that if there is is a torque imbalance, the generator will change its rotational speed. If, e.g., the load increases,

meaning that T_e increases, while the driving torque remains constant, then $\frac{d\omega}{dt}$ will be negative and the generator will decelerate. In this way, kinetic energy is converted to electrical energy to supply the load increase [7], [10].

2.1.1 Generation Characteristics

As described in the previous section, a stable operation of a turbine must have a power-speed characteristic such that the mechanical power increases when the speed decreases, and inversely the mechanical power has to decrease when the speed increases. To regulate the power and speed, turbine governors are used to achieve the desired characteristic. A typical turbine governor control can be expressed as

$$\Delta P_m = -\frac{1}{R}\,\Delta\omega \tag{2.2}$$

in steady state. The power difference ΔP_m is the change in turbine mechanical power output, $\Delta\omega$ is the change in speed and R is known as the regulation constant [10]. The inverse of R, namely $\frac{1}{R}$, is known as the speed-droop coefficient or simply as the droop [14]. Since the speed of synchronous generators is proportional to the grid frequency, (2.2) can be rewritten as

$$\Delta P_m = -\frac{1}{R}\,\Delta f, \tag{2.3}$$

using per-unit quantities in (2.2) and (2.3). Figure 2.1 shows a standard steady state speed-droop characteristic of a turbine with slope $-R$. This is also the steady state frequency power relation. In this figure, the turbine is operational within the interval of P_{min} to P_{max}, being limited at the bottom by technical parameters such as burner stability in coal plants and at the top by thermal and mechanical considerations [14]. At P_{max}, the turbine power production does not increase any longer with decreased frequency.

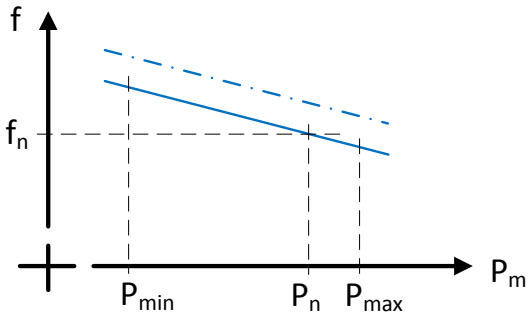

Figure 2.1: Steady state speed-droop characteristic for a turbine-governor

In a real power system, many generating units are operating synchronously at the same frequency. To obtain the complete generation characteristic of the whole system, the speed-droop characteristics of all individual turbines are added. During normal operation of a power system, many turbines will not be loaded to their maximum level. This means that there is a reserve generating capacity from generators that are online, but operating at partial loading. This reserve is called the spinning reserve, which is defined as the difference between the sum of the turbine power ratings and total system load. Due to different loading levels of the turbines and the spinning reserve, the complete system generation characteristic will be a non-linear curve as the one shown in Figure 2.2. For practical reasons, this curve may be linearized in the vicinity of the operating point when analysing small frequency and power fluctuations. It can be noted that the droop, the slope of the generation characteristic, becomes infinite at P_{max}, as is shown by the dashed line. This would be the theoretical case when all generators are operating at their maximum power output level and

the spinning reserve is down to zero. In reality, however, power plants usually have a frequency dependent so-called curled-back characteristic, which makes the total speed-droop curve have this feature as well [14].

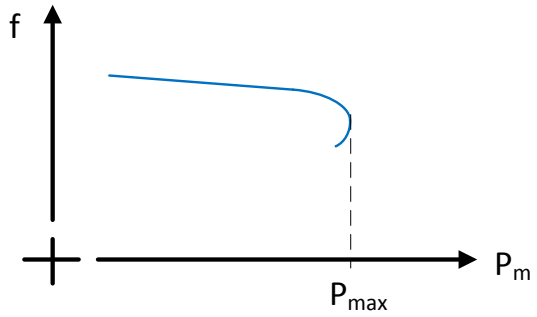

Figure 2.2: System generation characteristic.

2.1.2 Primary Control

The main goal of primary control is to stop the change in frequency and make the power system reach a new steady state frequency. When a power system event occurs which affects the frequency, e.g. the loss of a generator or a load step, the very first thing to happen is that the rotational speed of the turbine-generator is affected by a transient extraction or addition of kinetic energy. When the frequency changes, the primary control comes into action. First, the speed deviation is sensed by the speed-governing system. The speed deviation signal will be passed through a PI regulator and sent as a control signal to actuate the valves or gates of the turbine [12]. This will increase or decrease the turbine action, depending on whether the frequency has dropped or raised. The integral action will make the system reach a new steady state, though at an off-nominal frequency due to the droop characteristic according to Figure 2.1.

Normally, the aggregated load of a power system will change according to the frequency, i.e., it is not a constant power load. The frequency sensitivity of the load is opposite to that of the turbine-governor characteristic, so that when the frequency decreases, the load demand will decrease and vice versa. Most commonly, the generation frequency dependency is much larger than the load frequency sensitivity, meaning that the change in power generation is much larger than the change in load demand when subjected to equal frequency deviations [14]. As indicated in Figure 2.2, an increase in total system power is only possible when there is a spinning reserve, i.e., when there are generating units operating at partial load. These partially loaded generators should ideally be spread out to all areas of a power system in order not to overload transmission lines when an area of the power system requires extra power from a spinning reserve located far away. In an interconnected system, according to the solidarity principle, each control area is therefore expected to provide a spinning reserve proportional to its share in the whole synchronised area.

Production units participating in primary control are controlled with a dead band for their frequency set points. Different grid codes put different requirements on how fast part of, and the whole, spinning reserve should be activated. Generally, the part of the spinning reserve which is available for primary frequency control should be fully accessible within 15-23 seconds [14]. In the Nordic grid code [16], it is stipulated that the primary reserve should always be activated when the frequency reaches 49.9 Hz. In the event of a frequency drop to 49.5 Hz, 50% of the primary reserve power is obliged to be regulated upwards within 5 seconds, and 100% within 30 seconds. If, e.g., a significant production unit is unexpectedly lost, there will be a rapid reduction in frequency. Initially, rotor swings in generators will occur since kinetic energy is extracted from

all synchronously operating turbine-generators. The power support achieved in this way will be brief and likely insufficient, depending on the size of the outage. When the grid frequency drops, the primary control is activated and the spinning reserve power should be fully online in less than half a minute, as can be seen in Figure 2.3.

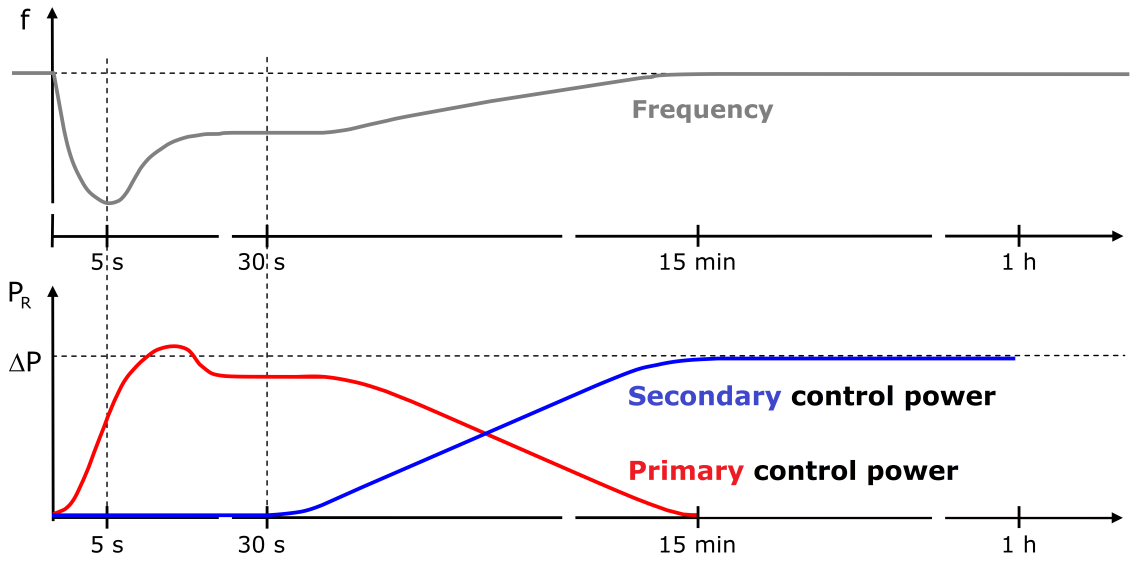

Figure 2.3: Schematic of the action of the primary and secondary frequency control. The upper Figure shows a possible frequency response in case of a generation outage. The lower Figure shows the working of the primary control power (red curve) and the secondary control power (blue curve). Figure adopted from [11].

2.1.3 Secondary Control

Follwing the action of a successful primary frequency control, the grid frequency will be stable at an off-nominal frequency. The main task of the secondary control is to take care of this frequency deviation and bring back the steady state frequency to its nominal value, as shown in Figure 2.3. At the same time, it can be seen that the secondary control restores the primary frequency control reserve. Finally, the secondary control is also responsible for guaranteeing that scheduled tie line power interchanges are maintained. This is important since is assures that each control area of an interconnected power system absorbs its own load changes, which is called the non-intervention rule. In such systems, secondary control is always decentralized since the regulator control loops are not able to sense where a power deficit occurs. Using centralized secondary control would therefore result in unwanted tie-line power flows, violating inter-operator agreements [14]. Secondary control is performed through altered power reference levels of turbine governors. This will result in the frequency-power curve of Figure 2.1 being moved up (dash-dotted line). Thereby, the power production will be able to meet the load level at nominal frequency, which is the desired goal of the load-frequency control. In the Nordic power system, automatic secondary control is not used. The means to regain nominal frequency is instead to manually adjust the power reference levels of production units, a procedure which is sometimes referred to as tertiary control. In the UCTE grid of the European continent, secondary control is handled automatically, so-called automatic generation control.

2.2 Wind Turbines and Generator Systems

Wind power plants use wind turbines to extract the power contained in the wind. The amount of power that can be extracted from the wind is equal to the power which is physically contained in the moving mass of the air, multiplied by the factor c_p. This is expressed as

$$P_{wind} = \frac{1}{2} c_p \rho A v_{wind}^3, \tag{2.4}$$

where ρ is the air density, A the area swept by the turbine and v_{wind} the wind speed. The constant c_p has a maximum theoretical value of 0.599, which is termed Betz limit after the discovery by Betz in 1926 [1], [14]. As can be seen in (2.4), wind power is proportional to the cube of the wind speed. This means that even small wind fluctuations will impact the generated power significantly. Another important quantity is the tip speed ratio λ, which is defined as

$$\lambda = \frac{v_{tip}}{v_{wind}} = \frac{R\omega}{v_{wind}}. \tag{2.5}$$

In this case, the blade tip speed v_{tip} and the wind speed v_{wind} are given in m/s, R is the turbine radius in m, i.e., the blade length, and ω is the turbine rotation in radians per second. Once again looking at (2.4), it is obvious that a high wind speed, a large turbine swept area and a high value of c_p will all lead to a high power being generated by the wind power plant. Among these parameters, c_p, which depends on λ, is the only one that can be controlled. Therefore, adjusting λ so that c_p reaches its maximum value is a natural strategy when operating a wind turbine. To do this, v_{tip} has to be adjusted and therefore this operational method called Maximum Power Point Tracking (MPPT) is primarily used by variable-speed wind turbines. Figure 2.4 shows the typical form of a $c_p(\lambda)$ curve, whose exact form differs between different wind turbines and is often determined through experimental set-ups.

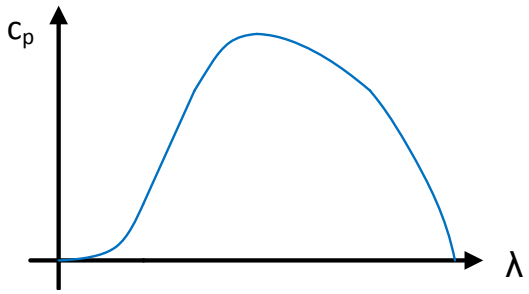

Figure 2.4: Typical form of a $c_p(\lambda)$ curve.

In addition to turbine speed control, the aerodynamic force of a wind turbine is controlled to help regulate the power production. This is especially applied to protect the wind turbine from too high wind speeds. During stormy weather conditions, wind turbines have to shut down and lock their blades in order not to be damaged due to too high mechanical stress. The aerodynamic control can be done in three different ways: stall control, pitch control and active stall control. Stall control is the simplest and most robust way of controlling the aerodynamic forces. In this case, the blades are mounted to the hub with a fixed angle towards the wind. The blades are designed in such a way that when the wind speed increases, the wind absorbing ability of the blades decrease and the rotor will stall above a given wind speed. In contrast to the passive stall control, pitch control offers an active way of controlling the aerodynamic force absorption. In such a configuration, the blades can be turned out of or into the wind, i.e., they can be pitched. This will change the angle of the blades, affecting how well they absorb wind. At wind speeds exceeding the construction limit

of the turbine, the blades pitch completely, minimizing the aerodynamic performance of the rotor and making it stop rotating. The third option of aerodynamic control is the active stall control. As the name indicates, the stall of the blades is actively controlled through pitching. At low wind speeds, the blades are pitched to achieve maximum efficiency and at excessive wind speeds, the blades are slightly pitched in the opposite direction of standard pitch control, making the blades stall further. Of these power control concepts, all three are used in combination with fixed-speed turbines whereas only pitch control is used with variable-speed turbines [1].

2.2.1 Fixed-Speed Wind Turbines

In spite of the benefits of adapting the turbine rotation and thereby controlling the tip speed ratio λ, fixed-speed wind turbines are the traditionally favoured wind power concept. An example of such a turbine-generator configuration is shown in Figure 2.5. A fixed-speed turbine operates at a nearly constant speed determined by the grid frequency and the gearbox ratio. The turbine is connected to an induction generator which can be of two types, with a squirrel-cage (short circuited) rotor or with a wound rotor. Of these two, the squirrel-cage rotor is the simplest construction, but the speed variability is limited to that of the slip of the induction machine. Using a wound rotor, the rotor resistance can be controlled, allowing a somewhat higher speed operating range. In either case, the connection between the turbine and the grid is rather stiff, which means that the transient torques caused by wind gusts will cause considerable gearbox wear. Furthermore, the stator of the induction machine may be equipped with two different sets of windings, one with eight poles used to operate at low wind speeds and one with four to six poles used during higher wind speed conditions. Apart from the limited speed elasticity, the main disadvantage of fixed-speed turbines using induction machines is their need for a magnetising current. This reactive current has to be drawn from the grid if it is not supplied by e.g. shunt capacitors. Still, fixed-speed turbines have been widely used due to their overall robust and simple construction and their cheap electrical components [1], [14].

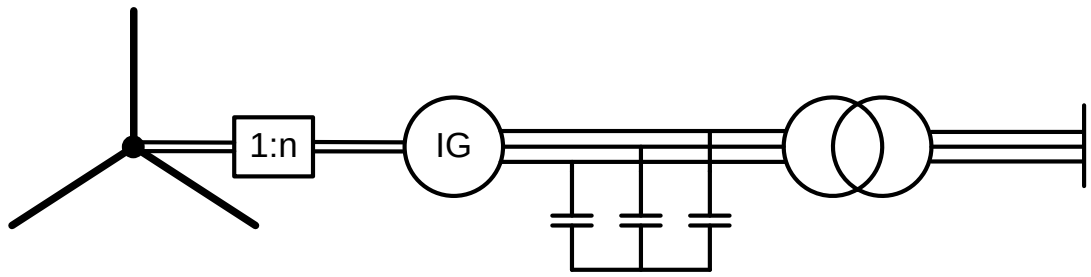

Figure 2.5: A fixed-speed wind turbine with a squirrel-cage induction generator.

2.2.2 Variable-Speed Wind Turbines

During the last decade, variable-speed wind turbines have gained favour and among newly installed turbines, they are almost exclusively chosen. The main reason for this is their better energy capture and thereby their better economic yield. To permit a varying speed, power electronic converters are added to the generator configuration. In this way, wind gusts are absorbed primarily by changes in the generator speed and in contrast to fixed-speed turbines, the generator torque is kept fairly constant. In addition to increased energy yield, the use of power electronics enables the wind turbine to control active and reactive power, which increases compliance to grid codes. Although the power electronic components give these benefits, they are also the main drawback of

this turbine configuration since they raise costs and construction complexity and possess inherent losses [1], [14].

The main variable-speed generator systems are the doubly-fed induction generator (DFIG) system and synchronous generators together with fully rated power converters. Fully rated converters may also be used to interface induction generators to the grid. In the DFIG concept, shown in Figure 2.6, an induction generator with a wound rotor is used. The stator is connected directly to the grid at system frequency. The rotor is connected to the grid via a back-to-back voltage source converter. This converter feeds the rotor windings at slip frequency, inevitably requiring slip rings. The basic operating principle is that the grid side converter controls the DC-link voltage and the machine side converter controls the active and reactive power through the rotor current components. Normally, the DC-link voltage is adjusted to ensure a converter operation at unity power factor. However, the power electronic converter allows the wind turbine to supply or absorb reactive power and thereby to help in voltage control, if required by the grid operator. In either case, the induction generator needs reactive power to be magnetised, which can be taken either from the grid or from the rotor. In subsynchronous operation, active power is fed to the rotor from the grid, and in supersynchronous operation in the opposite direction. In both cases, the stator will supply power to the grid. A DFIG wind turbine offers variable speed operation within a range that is determined by the power rating of the converter, normally being a fraction of about 30% of the generator rating. The cost of the power electronic equipment is thereby subject to the desired speed controllability, which allows for an economical and technical optimization [1], [14].

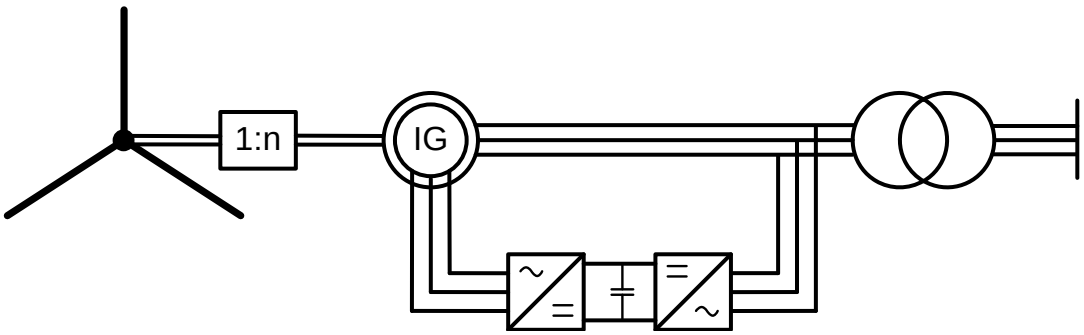

Figure 2.6: A variable-speed wind turbine with a doubly-fed induction generator (DFIG).

The second main configuration of variable-speed wind turbines is a synchronous generator interfaced to the grid via a frequency converter. Depending on whether or not the generator is of a multipole type, the configuration may exclude or include a gearbox. In this configuration, the frequency converter completely decouples the generator rotation from the grid frequency. Therefore, the converter has to be rated at the full power rating of the wind turbine. This is perhaps the main disadvantage of this set-up, since the cost increases compared to the DFIG. On the other hand, the clear benefit over the DFIG is that the generator does not need a magnetising reactive current. The fully rated converter provides full speed controllability as well as full control over active and reactive power. The output from the generator is first rectified to the DC-link and subsequently inverted to grid frequency, which allows for a completely synchronous operation of the generator. The synchronous generator may be of two different types, with a wound rotor or with permanent magnets. In case of a wound rotor, as in Figure 2.7, the excitation is provided by DC current fed to the rotor windings through slip rings or through a rotating rectifier. Using this gives the possibility of adjusting the magnitude of the induced emf in accordance with the generator rotation. In the case of permanent magnets, these provide the necessary excitation, which results in a higher efficiency. Two disadvantages of permanent magnet machines are costly magnetic materials and deterioration

of their magnetic properties when subjected to high temperatures, e.g. during a fault [1], [14].

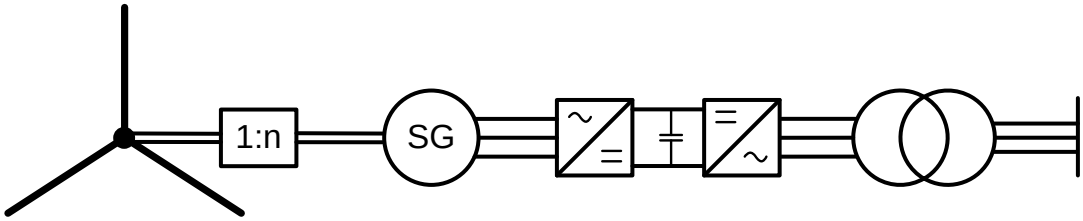

Figure 2.7: A variable-speed wind turbine with a wound rotor synchronous generator interfaced via a fully rated power electronic converter.

2.3 Operation of Wind Turbines

As was seen in Section 2.2, Maximum Power Point Tracking is the natural way to maximise the energy capture of a wind turbine. Such an operational strategy makes the wind turbines extract as much power as it possibly can for each given wind speed. This is the economically most beneficial method of operating a wind power plant, but when grid codes begin to put requirements on wind power to help in e.g. frequency regulation, other operational modes are required. If a frequency dip occurs in the grid and the wind turbine is expected to increase its power delivery, this will initially be done through an extraction of kinetic energy from the rotor, decreasing the turbine rotation. However, if additional power is needed to compensate the frequency dip, prior to the frequency dip the turbine has to be operated in a mode where not all the available wind energy is extracted. As a frequency dip occurs, the wind turbine should then be able to increase its energy capture up to the maximum available level, thereby providing as good frequency support as possible. Operational strategies like these are commonly referred to as deloading operation or delta operation and may be performed in different ways as described in the two following subsections.

2.3.1 Deloading Strategies

In [1], [15] and [19], four different deloading schemes are presented. These are: (i) limiting maximum power; (ii) absolute power reserve; (iii) relative power reserve; and (iv) power rate limitations. To limit the maximum power is equal to a derating of the wind turbine. This solely effects the turbine when its power production is close to the nominal power. The second alternative, an absolute power reserve, means that the available power is curtailed with a fixed amount whenever possible. Third, a relative power reserve provides a reserve equal to a fixed percentage of the available power, resulting in a lesser MW reserve at lower wind speeds. Last, the power rate limitations is a way to prevent the generated power from rising too quickly. Thereby, a certain power reserve will be available following wind speed increases. These four methods are illustrated in Figure 2.8.

2.3.2 Deloading Implementation

To actually implement the deloading concepts described in the previous paragraph, 2.3.1, the wind turbine has to be operated in a non-optimal operating point. According to [13] and [23], this can be done via under speeding, over speeding or by increasing the pitch angle. Taking Figure 2.4 as a starting point, it can naturally be redrawn with the turbine speed on the x-axis and the generated power on the y-axis for a band of different wind speeds within the medium wind speed range, i.e., wind speeds for which constant c_p control is applied (as described in Section 3.6 and illustrated in

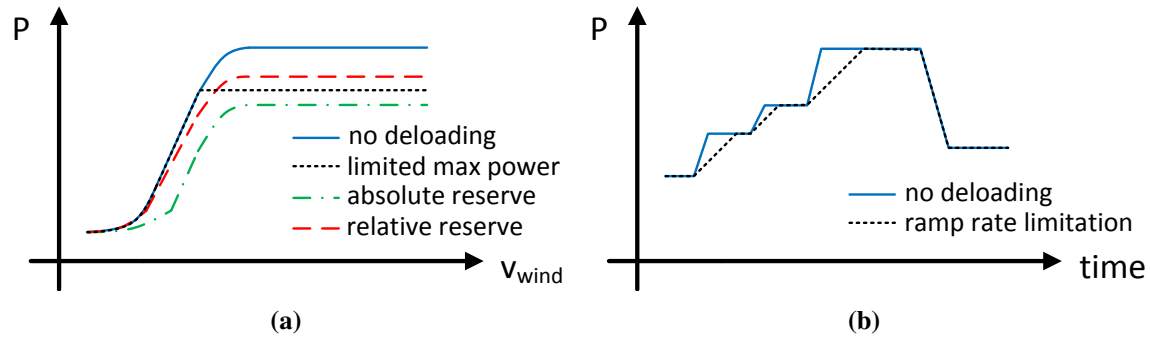

Figure 2.8: Illustration of different deloading options: (a) limtited maximum power, absolute and relative reserve; (b) ramp rate limitation.

Figure 3.4). This redrawn graph is shown in Figure 2.9 together with the MPPT line. Under speed operation means that the turbine operates at a speed lower than the one given by the MPPT mode, reducing the generated power. Analogously, over speed operation means that the turbine operates at a higher speed than the MPPT speed, which also leads to a power level lower than the MPPT. In either of these cases, there is a margin power available which can be utilized when needed. Under speeding is, however, not a favourable way of deloading a turbine since the available kinetic energy in the rotor decreases and thereby the ride through capabilities of a short wind speed decrease. In contrast, over speeding increases the stored kinetic energy in the rotor. Over speeding may only be implemented up to the nominal rotational speed.

The third way of implementing turbine deloading is to increase the pitch angle which leads to a less efficient wind capture and a lower generated power.

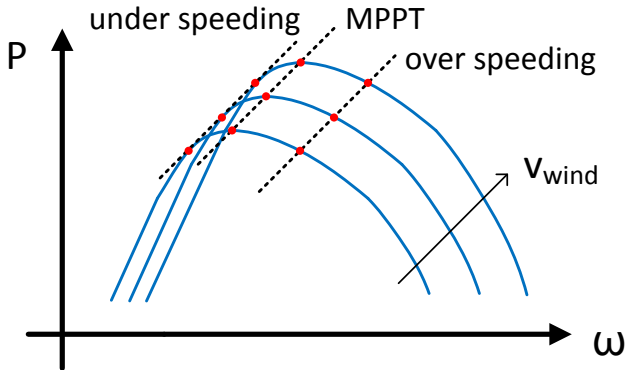

Figure 2.9: Wind turbine power as a function of the turbine speed for increasing wind speed within the medium wind speed range. Under and over speeding in comparison to MPPT operation.

Chapter 3

Default Wind Power Modelling in SIMPOW

In this thesis, the power system simulation software SIMPOW [17] is used. The main reason for the choice of software was that the previous work done by ÅF in [20] and [21] was performed in SIMPOW. Much of the basic structure of the models could therefore be utilized.

SIMPOW has a built-in model of a "full power converter wind turbine" (FPCWT). This model is used and has been modified and extended according to Chapters 4 and 5. However, in its default configuration it consists of the parts listed below, which interact according to the outline given in Figure 3.1.

- Wind turbine
- Synchronous generator
- PWM converter
- Shunt capacitor
- Speed control system
- Pitch control system
- AC voltage control system

Throughout this chapter, the wind power modelling in SIMPOW will be described, based on the SIMPOW manual [18].

3.1 Power Flow Calculation and Dynamic Simulation

Two of SIMPOW's main modules are the so-called optpow and dynpow modules. The optpow module does the initial steady state power flow calculation and the dynpow module the dynamic simulation. In optpow, the electrical state of the AC system is assumed to be symmetrical and sinusoidal at nominal frequency. The power system is therefore represented by a single phase model and electrical quantities described by positive sequence phasors. Running an optpow simulation gives the initial values necessary to perform a dynamic simulation with the dynpow module.

The dynpow module has two different modes, TRANSTA (short for transient stability) and MASTA (machine stability). In TRANSTA simulations, harmonics are neglected and only the fundamental frequency component is considered. The TRANSTA module primarily deals with power flows in the network, changes of relative rotor angles and electromechanical transients.

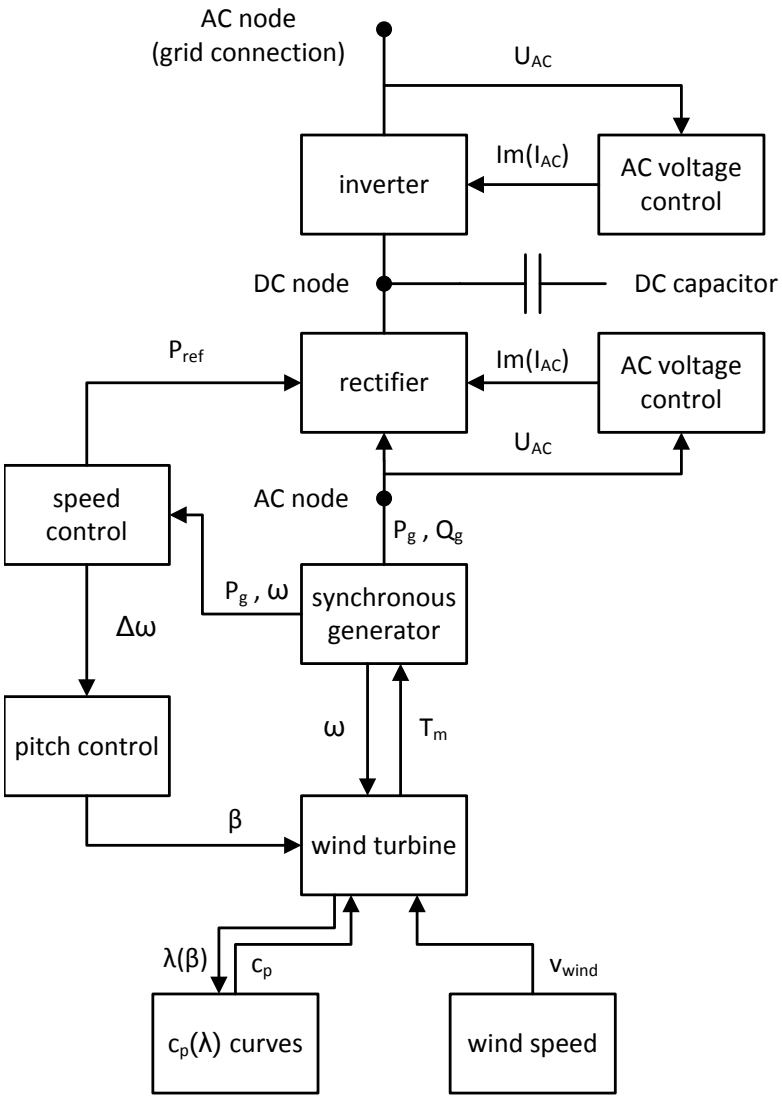

Figure 3.1: Block diagram of the SIMPOW FPCWT model and main communication between its modules. Figure adopted from [18].

It uses phasor representation and symmetrical components. The MASTA module on the other hand uses instantaneous values through dq0 components and is used to study the exact behaviour of voltages and currents when the electrical state cannot be assumed to be sinusoidal, e.g. in case of saturation and resonance phenomena. The FPCWT model available in version 11.0.008 of SIMPOW (used in this project) is only implemented for TRANSTA simulations [18].

3.2 Wind Turbine Modelling

The FPCWT model in Figure 3.1 includes a module for the turbine. This module has as its inputs the turbine rotation ω, the pitch angle β, the coefficient c_p and the wind speed v_{wind}. As outputs it gives the tip speed ratio λ and T_m, the mechanical torque exerted in the generator shaft. The ratio λ is calculated by (2.5) and T_m is obtained by dividing the mechanical power by the angular speed ω, which in accordance with (2.4) gives that

$$T_m = \frac{P_{wind}}{\omega} = \frac{\frac{1}{2} c_p \rho A v_{wind}^3}{\omega}$$

3.3 Wind Farm Modelling

To decrease computational costs, a wind farm may in SIMPOW be modelled as a single aggregated turbine instead of many individual turbines. During a simulation, most quantities are in per-unit values and these may be scaled simply by changing the base power. However, to be able to use normal $c_p(\lambda)$ curves, the turbine blade length R and the nominal rotational n_n speed have to be adjusted. In SIMPOW this is done by calculating $R_{farm} = R_{turb} \cdot a$ and $n_{n,farm} = n_{n,turb}/a$. The constant a is obtained as $a = \sqrt{S_{n,farm}/S_{n,turb}}$, where $S_{n,turb}$ and $S_{n,farm}$ are the rated powers of the turbine and the wind farm respectively [18].

3.4 Synchronous Generator

In SIMPOW, synchronous generators may be modelled in basically four different ways:

1. with one field winding, one d-axis damper winding and two q-axis damper windings, with or without saturation
2. with one field winding, one d-axis damper winding and one q-axis damper winding, with or without saturation
3. with one field winding but no damper winding, with or without saturation
4. as a constant voltage source behind a transient reactance

The standard configuration of the FPCWT module utilizes a synchronous machine model of the second type, i.e., with a field winding, one d-axis and one q-axis damper winding, and excludes saturation.

There are also many different exciter models included in SIMPOW. Nonetheless, the default FPCWT configuration, uses a constant field voltage. For simplicity, this synchronous machine configuration is also the one used in this thesis work.

3.5 Power Electronic Converter

The power electronic converter of a wind turbine with a fully rated converter consists of a rectifier and an inverter, normally PWM converters. The FPCWT model in SIMPOW uses a simple representation of the rectifier and the inverter, neglecting the actual PWM switching. Figure 3.2 illustrates the function of the converter model. In this model, the active power through the series reactor is equal to the injected power minus the no-load losses P_L.

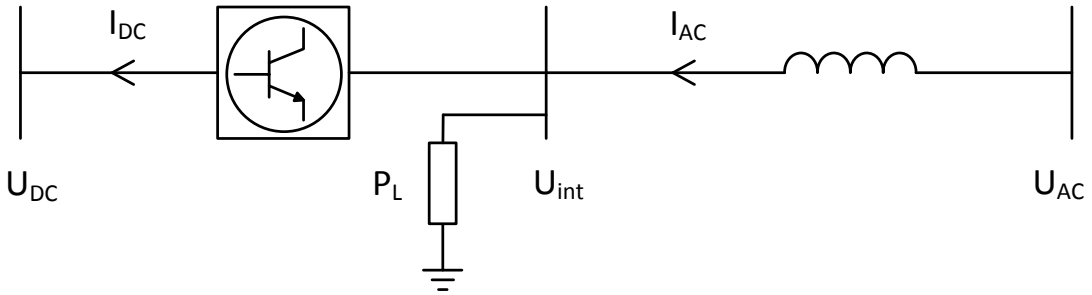

Figure 3.2: PWM converter model in SIMPOW. Figure adopted from [18].

Independent of it being set as a rectifier or an inverter, the PWM model controls the internal AC bus voltage U_{int} so that the real and imaginary parts of the AC current are according to

$$\mathrm{Re}(U_{int}) = \mathrm{Re}(U_{AC}) + X \cdot \mathrm{Im}(I_{AC})$$

$$\mathrm{Im}(U_{int}) = \mathrm{Im}(U_{AC}) - X \cdot \mathrm{Re}(I_{AC}).$$

When the converter operates in rectification mode, the real part of the AC current is controlled by an internal PI regulator so that the active power drawn at the AC bus is equal to the active power reference given by the speed controller, cf. Figure 3.1. This is simplified as

$$\mathrm{Re}(U_{AC}) \cdot \mathrm{Re}(I_{AC}) + \mathrm{Im}(U_{AC}) \cdot \mathrm{Im}(I_{AC}) = P_{AC} = P_{ref}. \tag{3.1}$$

In inverter mode, another internal PI regulator controls $\mathrm{Re}(I_{AC})$ to maintain the set value of the DC link voltage. Using (3.1), the following expression is obtained:

$$P_{DC} = P_{AC} - P_L = \mathrm{Re}(U_{AC}) \cdot \mathrm{Re}(I_{AC}) + \mathrm{Im}(U_{AC}) \cdot \mathrm{Im}(I_{AC}) - P_L = U_{DC} \cdot I_{DC}. \tag{3.2}$$

From (3.2), $\mathrm{Re}(I_{AC})$ can then be found as:

$$\mathrm{Re}(I_{AC}) = \frac{U_{DC,ref} \cdot I_{DC} - \mathrm{Im}(U_{AC}) \cdot \mathrm{Im}(I_{AC}}{\mathrm{Re}(U_{AC})}. \tag{3.3}$$

Finally, the imaginary part of the AC current, which is needed in (3.1) and (3.3), is given by the AC voltage control as described in Section 3.8 [18].

3.6 Speed Control

The speed controller is an integral component of every variable-speed wind turbine. Its main purpose is to keep the operating point of the wind turbine at $c_{p,max}$, cf. Figure 2.4. In the speed controller, first the speed reference ω_{ref} for Maximum Power Point Tracking is calculated. The reference value ω_{ref} is subtracted from the actual turbine speed ω to obtain the speed deviation $\Delta\omega$. The deviation is fed trough a PI controller and thereafter multiplied by ω. Finally, this signal is low-pass filtered and limited in magnitude, giving the reference active power P_{ref} which is sent to the rectifier, as shown in Figure 3.1 and 3.3.

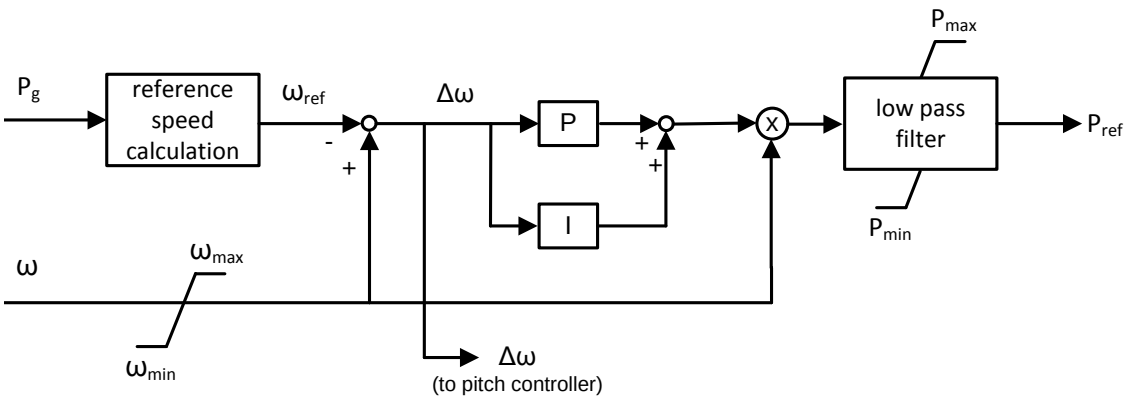

Figure 3.3: Schematic of the unregulated wind turbine speed controller system. Figure adopted from [18].

As stated, the speed controller aims at keeping the turbine operating point at $c_{p,max}$. This is possible within a certain wind speed range. At too high wind speeds the turbine will not be able to operate at its optimal point since the blades are pitching to prevent generator overload. At too low wind speeds, maintaining an operation at $c_{p,max}$, and consequently at λ_{max} would require a tip speed lower than the turbine minimum rotational speed. Therefore, at too high wind speeds as well as too low, the operating point moves away from $c_{p,max}$. The general turbine performance is illustrated in Figure 3.4. The low wind speed range in this figure approximately corresponds to wind speeds lower than 6 m/s. The high wind speed range begins at rated wind speed and continues up until the turbine completely has to shut down for security reasons.

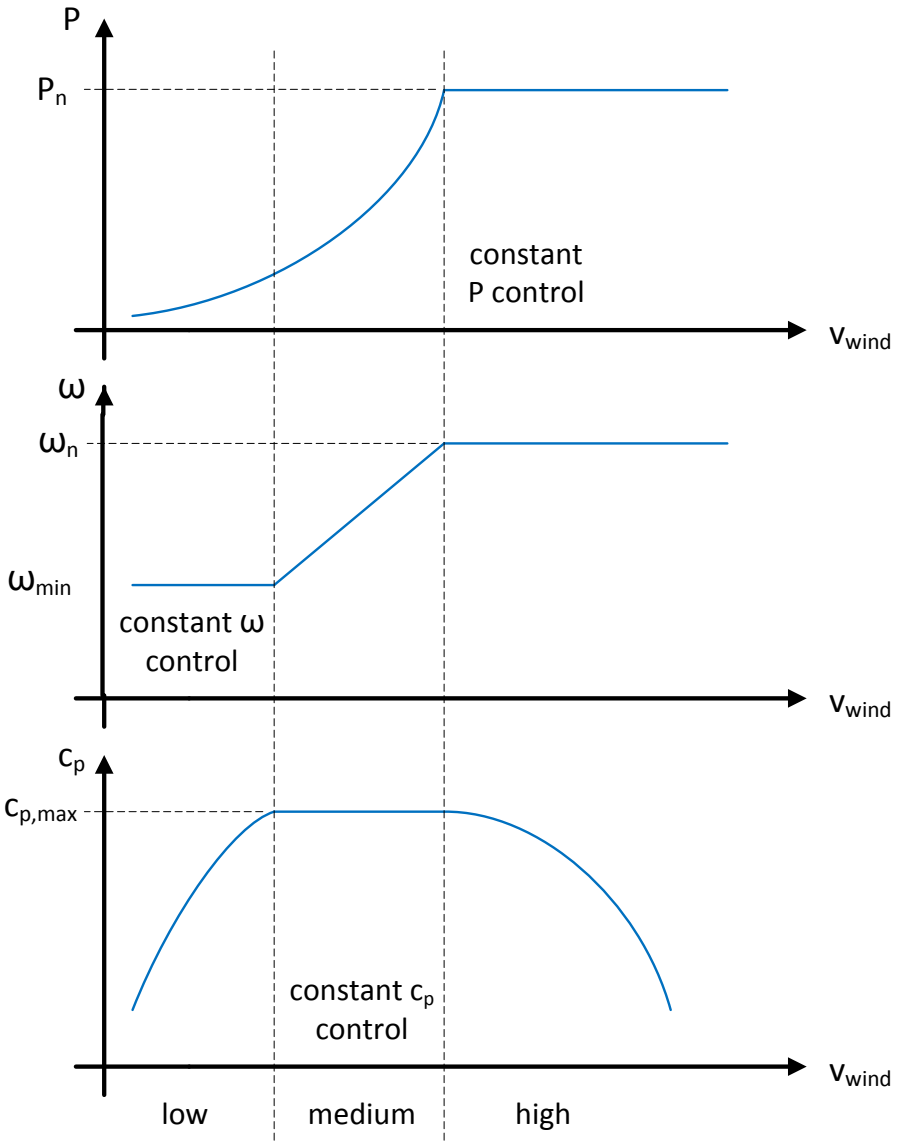

Figure 3.4: Overall wind turbine operation as governed by the speed and pitch controllers. Figure adopted from [18].

3.6.1 Default Calculation of the Speed Reference

The core of the speed controller system is the calculation of ω_{ref} from the generated power P_g, which is done according to

$$\omega_{ref} = A_0 + A_1 P_g + A_2 P_g^2, \tag{3.4}$$

where A_0, A_1 and A_2 are coefficients determined so that the turbine will operate at $c_{p,opt}$. To determine the coefficients, we start from (2.5), rewriting it as

$$\lambda = \frac{v_{tip}}{v_{wind}} = \frac{\omega R}{v_{wind}} \Leftrightarrow \omega = \frac{\lambda}{R} \cdot v_{wind}. \tag{3.5}$$

If we use per-unit quantities instead of physical units, (3.5) becomes

$$\omega_{pu} = \frac{\lambda}{\omega_n R} \cdot v_{wind}, \tag{3.6}$$

where ω_n is the nominal rotation speed used as speed base value. In optimal operation, $\lambda = \lambda_{opt}$ and therefore (3.6) may be expressed as

$$\omega_{pu} = \frac{\lambda_{opt}}{\omega_n R} \cdot v_{wind} = K_1 \cdot v_{wind}, \tag{3.7}$$

where K_1 is a constant. In a similar manner, the constant K_2 is obtained from (2.4) expressed in per-unit quantities. Neglecting losses in the wind power plant we get

$$P_{wind,pu} = P_{g,pu} = \frac{\frac{1}{2} c_p \rho A}{S_n} \cdot v_{wind}^3, \tag{3.8}$$

with the nominal power S_n used as base power. In optimal operation, $c_p = c_{p,opt}$ and (3.8) may be rewritten as

$$P_{g,pu} = \frac{\frac{1}{2} c_{p,opt} \rho A}{S_n} \cdot v_{wind}^3 = K_2 \cdot v_{wind}^3. \tag{3.9}$$

In order to derive the three coefficients A_0, A_1 and A_2, three equations are needed. Combining (3.4), (3.7) and (3.9) for three different wind speeds in the medium wind speed range of Figure 3.4, we get the following system of equation:

$$K_1 \begin{bmatrix} v_{wind,1} \\ v_{wind,2} \\ v_{wind,3} \end{bmatrix} = \begin{bmatrix} 1 & K_2 \cdot v_{wind,1}^3 & K_2^2 \cdot v_{wind,1}^6 \\ 1 & K_2 \cdot v_{wind,2}^3 & K_2^2 \cdot v_{wind,2}^6 \\ 1 & K_2 \cdot v_{wind,3}^3 & K_2^2 \cdot v_{wind,3}^6 \end{bmatrix} \begin{bmatrix} A_0 \\ A_1 \\ A_2 \end{bmatrix} \tag{3.10}$$

from which the coefficients are determined. The wind turbine is able to operate at $c_{p,opt}$ for all three wind speeds within the medium range, and one of them should preferably give nominal rotational speed. In this interval, the pitch angle should normally be zero and therefore K_1 and K_2 are calculated for the $c_p(\lambda)$ curve corresponding to $\beta = 0°$. Under these conditions, rated wind speed will give rated rotational speed and rated power, resulting in (3.7) and (3.9) giving

$$\begin{cases} K_1 = \dfrac{1}{v_{wind,n}} \\ K_2 = \dfrac{1}{v_{wind,n}^3} \end{cases} \tag{3.11}$$

as explained in [18]. In this thesis, a wind turbine model with a rated wind speed of 12 m/s has been used. If we insert this value in (3.11) and thereafter solve (3.10) with additional wind speeds 6 and 9 m/s, we receive the following values:

$$\begin{bmatrix} K_1 \\ K_2 \end{bmatrix} = \begin{bmatrix} 0.083333 \\ 0.000579 \end{bmatrix}, \qquad \begin{bmatrix} A_0 \\ A_1 \\ A_2 \end{bmatrix} = \begin{bmatrix} 0.370047 \\ 1.098151 \\ -0.468198 \end{bmatrix}$$

Lastly, the plotted speed reference curve is shown in Figure 3.5.

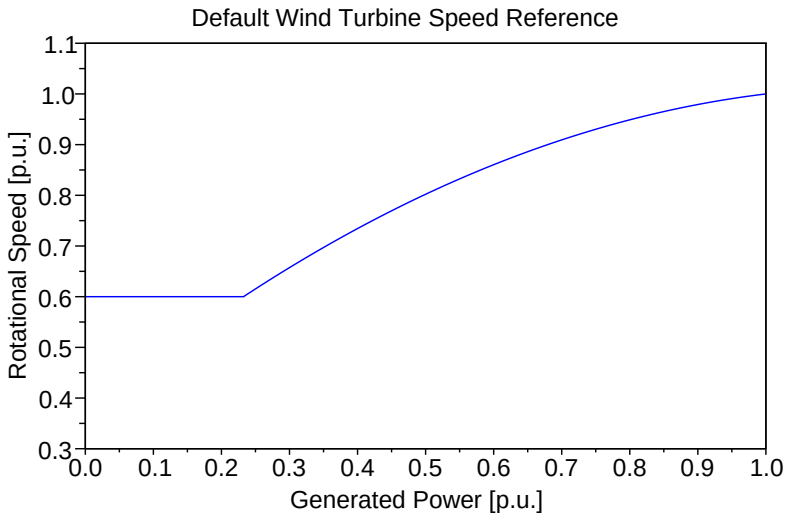

Figure 3.5: Speed reference curve for a wind turbine with a rated wind speed of 12 m/s, using the default speed controller in SIMPOW.

3.7 Pitch Control

In default operation, the objective of the pitch control system is to protect the turbine from generator overload and too high mechanical stress in case of strong winds. This means that at wind speeds exceeding rated wind, the pitch control will start pitching the blades to restrict the produced power and the rotational speed to their respective maximum values, as is seen in Figure 3.4.

The function of the pitch controller is shown in Figure 3.1. Its input signal is the speed deviation calculated by the speed controller. The speed deviation $\Delta\omega$ is fed to a PI regulator as shown in Figure 3.6. The output from the PI controller is then added to the pitch controller offset β_0 and finally low-pass filtered as well as limited in magnitude. The output of the pitch controller is the pitch angle which is fed to the wind turbine module. In simulations that are run with the default pitch controller, β_0 is set to -1. However, in the SIMPOW model this does not mean that the blades have an actual pitch angle of $-1°$, since the pitch angle minimum limit $\beta_{min} = 0°$ [18].

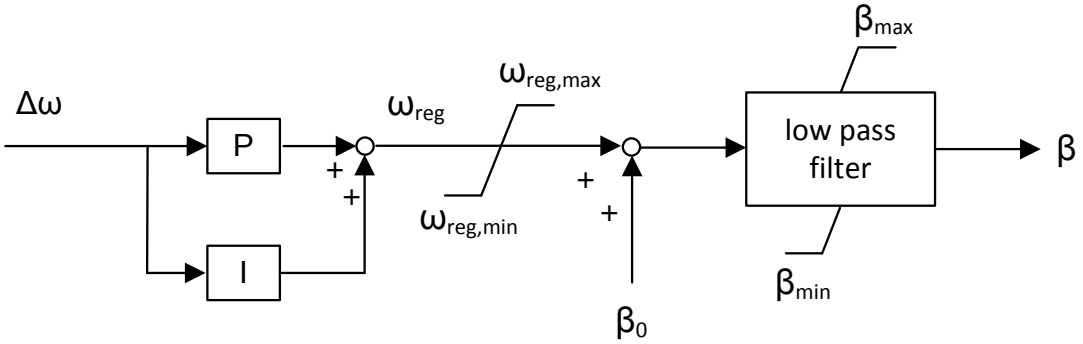

Figure 3.6: Schematic of the unregulated wind turbine pitch controller system. Figure adopted from [18].

3.8 AC Voltage Control

The objective of the AC voltage control is to give the imaginary part of the AC current required by the PWM converter model. With the imaginary current, the reactive power is controlled at the AC node of each converter. The voltage controller is a plain PI regulator, see Figure 3.7, taking as its input the voltage deviation $\Delta U_{AC} = U_{AC} - U_{AC,ref}$ and giving as output the reference value of Im(I_{AC}). In [18], Im(I_{AC}) is also identified as the q-axis current I_q.

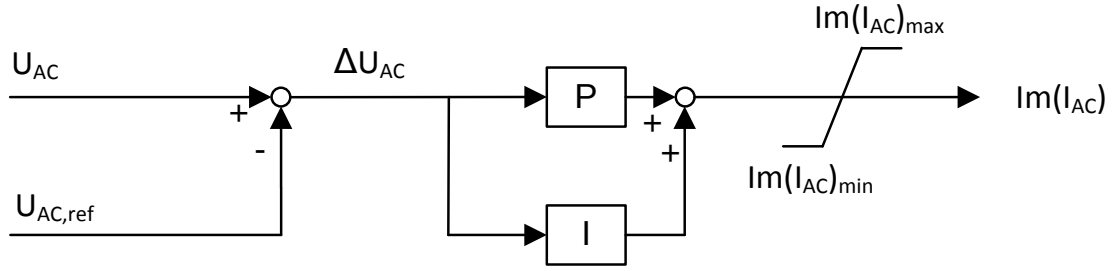

Figure 3.7: AC voltage control of PWM converters in SIMPOW. Figure adopted from [18].

3.9 Wind Data

In the dynpow simulation mode of SIMPOW, dynamic simulations with the FPCWT model may be run with an arbitrary wind series. The wind series should be given in the form of a table which supplies the wind speed value to the turbine module of Figure 3.1. The wind data used in this thesis work is taken from [21]. In that report, the original wind data comes from a wind power test facility operated by Chalmers University of Technology. The wind data has a resolution of one second. Out of the measured wind data, a selection was made in [21] to find two different wind series, one that corresponds to normal wind speed variations and one to extreme wind speed variations. These wind series are sometimes simply called normal and extreme wind, though it is always the wind fluctuations that are meant to be normal or extreme. The wind series were also processed to give wind data that better corresponds to: (i) the average wind exerted on the whole rotor; and (ii) the average wind exerted on a whole wind farm.

Chapter 4

Wind Turbine Regulators for Frequency and Power Smoothing Control

This chapter presents three different ways to control a wind turbine to improve the grid frequency. The first is the *frequency control* or *f-reg* developed by ÅF. The second is the *active power feedback control* or *P-reg* which has been developed in this thesis. The third method, which also is a result of this thesis, combines the two previous and is called the *combined frequency and active power feedback control* or *c-reg*.

4.1 Frequency Regulator (f-reg)

The most intuitive way to accomplish frequency regulation for any kind of power plant is to measure the off-nominal frequency deviation and use this as input to a control system. This is also the method that has been implemented by ÅF in [20] and it is used for comparison in this thesis. The regulator consists of a frequency measurement, from which the frequency deviation is fed through a proportional controller. In the literature, e.g. [5], [6] and [15], this is known as droop control, in analogy with conventional turbine governors and Equation (2.3). In the speed controller shown in Figure 4.1, the droop control signal is subtracted from the optimal power order. In the pitch controller shown in Figure 4.2, it is instead added to the pitch angle. Note that the value of the proportional gain of the frequency error is different in the pitch controller and the speed controller, though always positive. In this way, the power order from the speed controller will be increased when the grid frequency is below its nominal value, at the same time as the pitch angle will be decreased, and vice versa in case of too high frequencies.

4.2 Active Power Feedback Regulator (P-reg)

The prerequisite for the wind power controller to be developed in this thesis was that it should be based on a measurement of the actual generated power of the wind turbine. This power measurement was to be used as a feedback signal to a regulator in order smooth out the power when subjecting the turbine to fluctuating wind.

The initial idea was to compare the generated power P_g to a set point value P_{set} and try to maintain the set point value as the actually produced power. That is, when the generated power is higher than the set point, the turbine should decrease its power generation and when the generated power is lower than the set point, the turbine should increase its power generation. This is the simple starting point of the regulator model development.

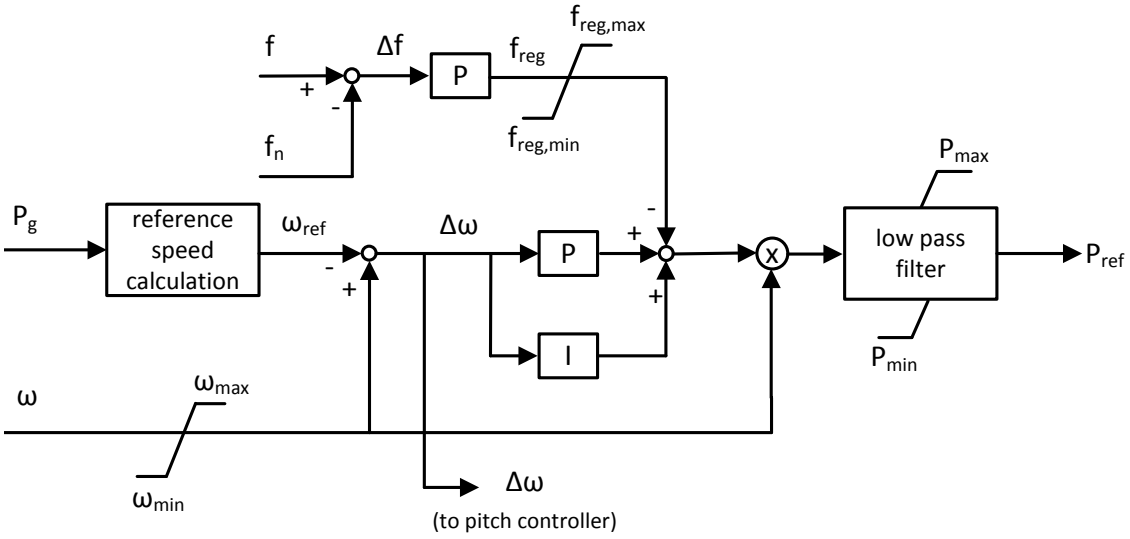

Figure 4.1: Schematic of the wind turbine speed controller featuring frequency control.

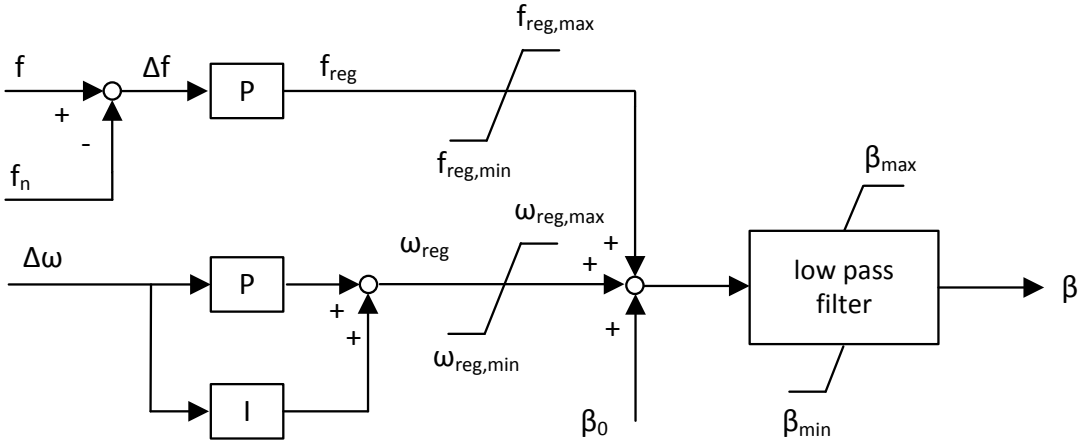

Figure 4.2: Schematic of the wind turbine pitch controller featuring frequency control.

To incorporate the power set point in a regulator to control the turbine power, the difference between P_g and P_{set} is calculated and multiplied by a constant. In the speed controller, this term is thereafter subtracted from the optimal power order value. If $P_g > P_{set}$, the power order is decreased, and if $P_g < P_{set}$, the power order is increased. Figure 4.3 shows this increased functionality of the speed controller. Likewise, the power deviation is fed to the pitch controller where it is added to the usual pitch angle, cf. Figure 4.4. If $P_g > P_{set}$, a positive contribution will be given to β. If, on the contrary, $P_g < P_{set}$, a negative contribution will be given to β. In this way, both the speed and the pitch controller are influenced to make the generated power more even, which will cause smaller wind induced frequency variations as long as the load and generation level from other power plants are constant.

4.2.1 Calculation of the Power Set Point

The next step is to find a way to determine the set point. Using a fixed set point is the easiest way to approach this, though very ineffective. To secure the operation of the wind turbine, a fixed set point would have to be set lower than the power level corresponding to the lowest forecasted wind speed. This would, however, be economically intolerable since considerable amounts of “free”

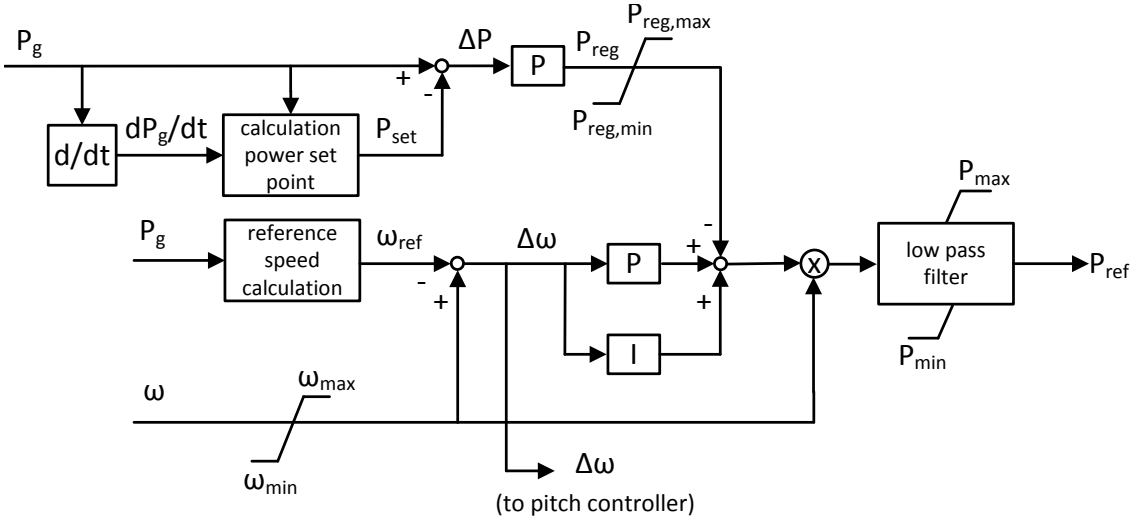

Figure 4.3: Simplified block diagram of the wind turbine speed controller featuring active power feedback control.

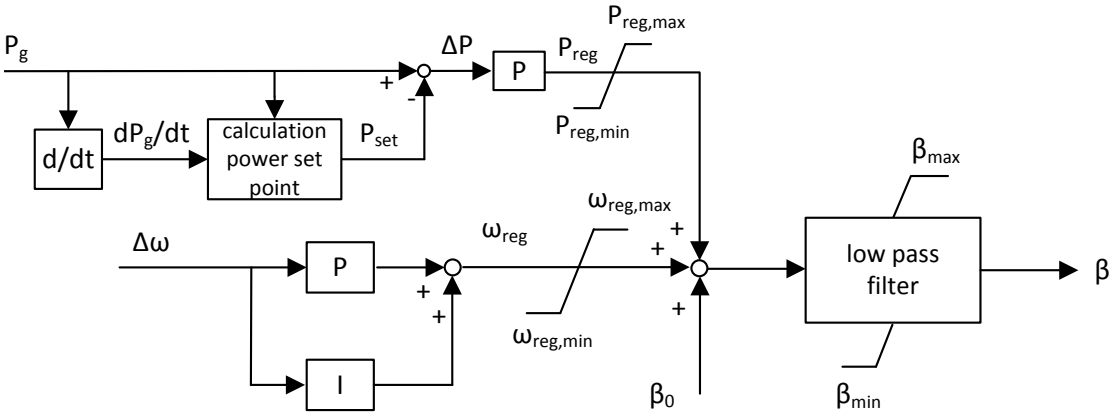

Figure 4.4: Simplified block diagram of the wind turbine pitch controller featuring active power feedback control.

energy would be wasted. On the other hand, setting the reference value higher than the minimum level would cause operating problems when the wind speed falls below a level corresponding to the power set point. In such cases, the turbine moment of inertia would render a temporarily maintained power output possible, though only for a very limited time. Alternatively, if the turbine operates with a pitch angle offset, the pitching of the blades could be reduced to allow a higher power output. In any case, if the pitch angles decreases to zero and rotational energy is extracted, eventually the turbine will slow down. This makes it require more energy to regain speed and will possibly cause the turbine rotation to stop if too much rotational energy is converted to electric energy. To solve this, a variable power set point was introduced.

The intention with the variable power set point is to get a reference that follows slow variations of the generated power but dampens fast peaks and valleys. Finally, the model shown in Figure 4.5 was obtained. First, the time derivative of the produced electric power, $\frac{dP_g}{dt}$, is calculated, low-pass filtered and limited with respect to its maximum and minimum permitted values. The power set point initial value $P_{set}(0)$ is set equal to the initial power production $P_g(0)$. During the simulation the power set point is adjusted in accordance with the time derivative of P_g, subjected to the following conditions.

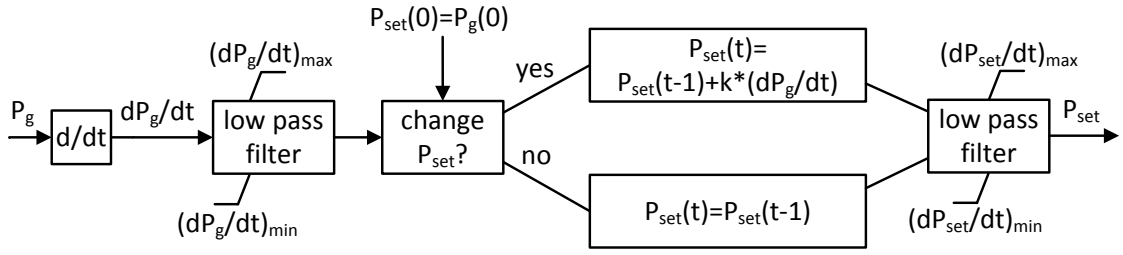

Figure 4.5: Block diagram showing the calculation of the variable power set point.

- if $(P_g > P_{set})$ & $(\frac{dP_g}{dt} > 0)$, P_{set} is increased
- if $(P_g > P_{set})$ & $(\frac{dP_g}{dt} < 0)$, P_{set} is left unchanged
- if $(P_g < P_{set})$ & $(\frac{dP_g}{dt} < 0)$, P_{set} is decreased
- if $(P_g < P_{set})$ & $(\frac{dP_g}{dt} > 0)$, P_{set} is left unchanged

P_{set} is changed by adding a term proportional to $\frac{dP_g}{dt}$ to it. The proportionality constant varies between three different values depending on the value of $\frac{dP_g}{dt}$. The purpose of this is to make P_{set} follow P_g in a satisfactory way.

If P_{set} reacts very slowly on changes in P_g, P_{set} will, e.g., not be able to follow a steep increase in P_g, possibly leading to a significant amount of unextracted wind energy. On the other hand, if P_{set} reacts on fast changes in P_g, the stabilizing effect on the generated power will not take place. In the case of decreasing wind speed, P_{set} also has to follow P_g adequately fast. Being too immobile, the set point will remain at a value higher than P_g, eventually causing the wind turbine rotation to stop since the control system tries to extract more power from the turbine than what is available from the wind.

Figure 4.6 show two examples of how the power set point curves may look. The upper part shows P_{set}, P_g and the wind speed for normal wind variations, and the lower part the same variables for extreme wind variations. Note however, that these plots only show the calculation of the power set point. P_{set} is not used to regulate the turbine performance in these plots.

4.3 Combined Frequency and Active Power Feedback Regulator (c-reg)

The regulation design as described so far does not actively participate in the frequency control, meaning that it does not sense frequency variations arising from load changes or changes in power generation from other power plants. To make an active frequency regulation possible, the active power feedback control has been combined with the frequency control from [20]. The combined control structure is outlined in Figure 4.7, the speed controller, and Figure 4.8, the pitch controller. Comparing these block diagrams with the ones for the active power feedback regulator, Figure 4.3 and 4.4, the difference is the additional subtraction of a control signal proportional to the frequency error. Such a control strategy normally results in a compromise between nominal frequency and an even power output. The c-reg method is tested in Chapter 6 together with the frequency control, f-reg, and the active power feedback control, P-reg.

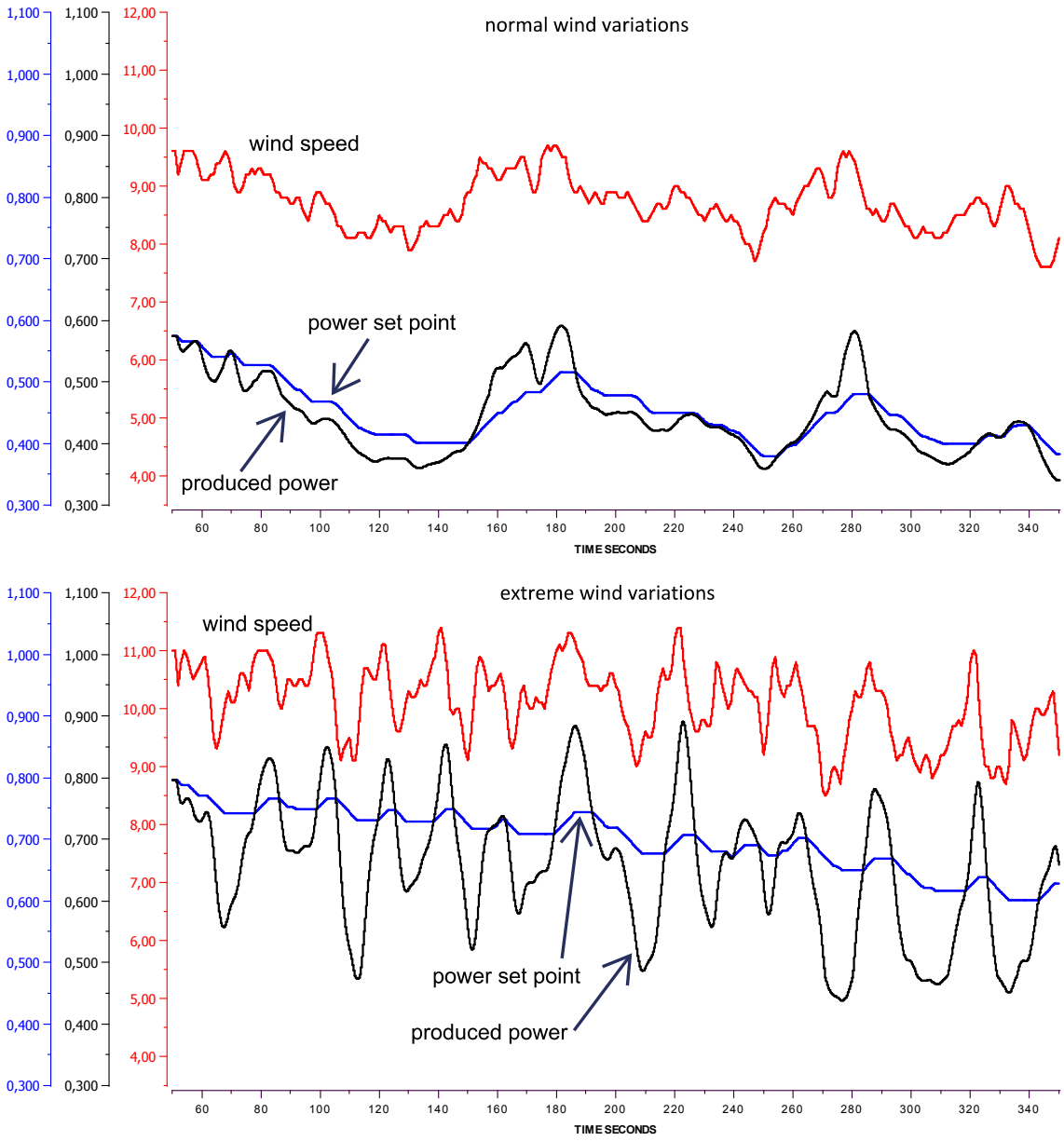

Figure 4.6: Power set point P_{set} plotted together with the wind speed and the produced power P_g of the unregulated wind turbine. Top figure: normal wind variation. Bottom figure: extreme wind variations.

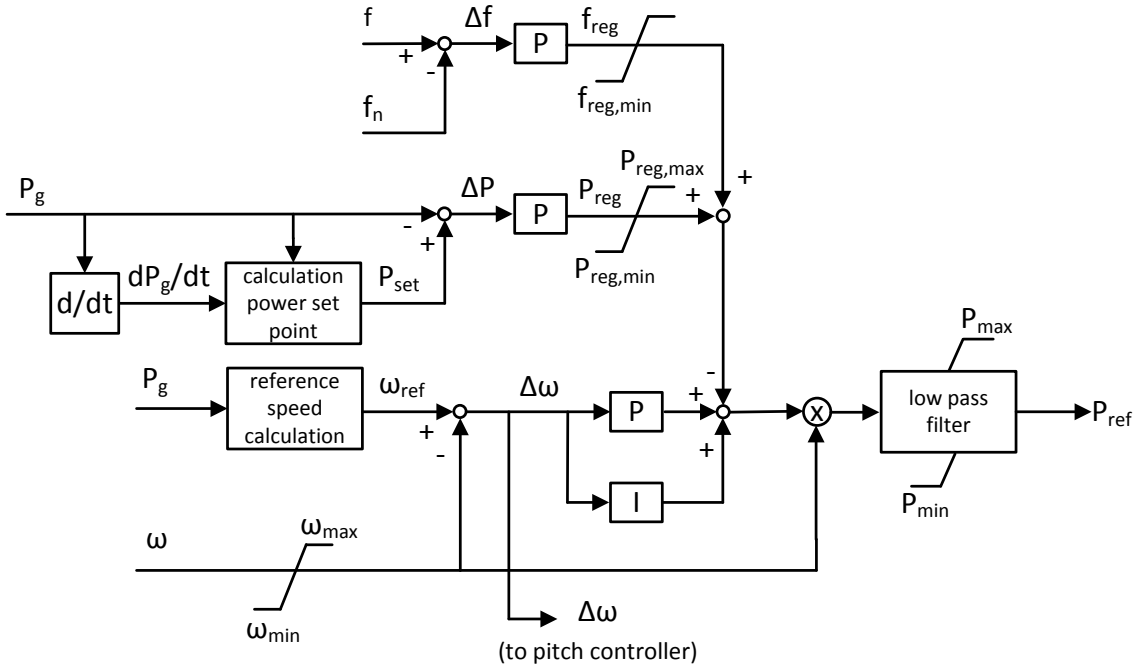

Figure 4.7: Simplified block diagram of the wind turbine speed controller featuring frequency control and active power feedback control.

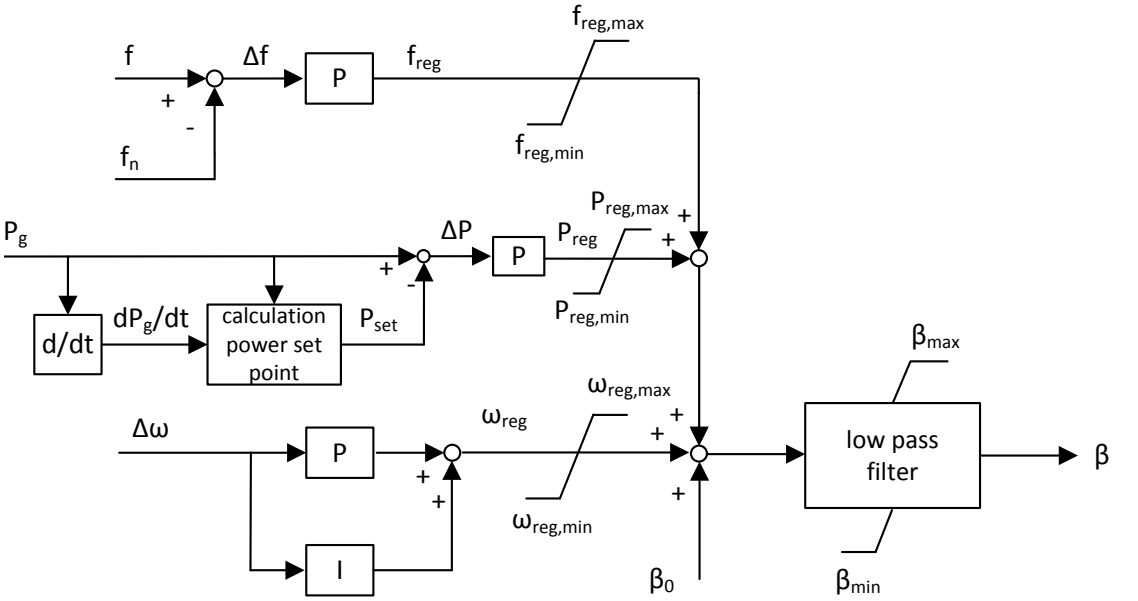

Figure 4.8: Simplified block diagram of the wind turbine pitch controller featuring frequency control and active power feedback control.

Chapter 5

Adapted Modelling of the Wind Power Speed Controller

As described in Chapter 1, this thesis work has taken its starting point in the work done by ÅF in [20] and [21]. These studies use the standard SIMPOW FPCWT model as explained in Chapter 3. Adding to this, [20] introduced the frequency controller outlined in Section 4.1. In the course of this thesis project, this model has been adapted on the following two areas:

1. better software implementation, which
   i) reduces unwanted oscillations in the beginning of each simulation
   ii) applies equal power bases to the generator, the turbine and the converters
2. more realistic speed reference curve, taking into account mechanical limitations of the tip speed

5.1 Modified Calculation of the Speed Reference

Returning to the speed controller of Section 3.6, it can be noted that it, up to rated values, assumes an injective relationship between the generated power and the turbine reference speed, cf. Figure 3.5. However, modern wind turbines tend to follow a λ_{opt} of around 9. This means that at a rated wind speed of 12 m/s, which was used in this project, the tip speed will become $v_{tip} = \lambda_{opt} \cdot v_{wind} = 9 \cdot 12 = 108$ m/s. While mechanical requirements normally limit the tip speed to 80 m/s [3], such a speed reference curve cannot be followed in reality. When imposing a limit of $v_{tip,max} = 80$ m/s, the optimal λ can only be maintained up until a wind speed of $v_{wind} = v_{tip,max}/\lambda_{opt} = 80/9 \approx 8.89$ m/s. Above this wind speed, the Maximum Power Point Tracking strategy must be abandoned and the operating point will inevitably move away from $c_{p,max}$.

When using the standard speed controller, produced power P_g will be proportional to the cube of the wind speed according to (3.9). However, implementing the more realistic speed controller means that c_p will not be kept constant up until rated wind. Therefore, P_g will be proportional to $c_p \cdot v_{wind}^3$ instead. As stated in the previous paragraph, nominal rotational speed will be reached already at a wind speed of 8.89 m/s. The produced power at this wind speed may therefore be expressed as

$$\frac{P}{P_n} = \frac{c_{p,max}}{c_{p,n}} \cdot \left(\frac{v_{wind}}{v_{wind,n}}\right)^3 \Leftrightarrow P = \frac{c_{p,max}}{c_{p,n}} \cdot \left(\frac{8.89}{12}\right)^3$$

in per-unit quantities. Using the fact that in nominal operation, $\lambda_n = v_{tip,max}/v_{wind,n} = 80/12 = 6.67$, the nominal value $c_{p,n}$ can be approximately read from the $c_p(\lambda)$ curves in Section 6.2.

Subsequent iterative simulations with rated, constant, wind speed resulted in $c_{p,n} = 0.4254$ for the data used in this project. Furthermore reading $c_{p,max} = 0.50$, the power produced at 8.89 m/s wind speed could be determined to

$$P = \frac{c_{p,max}}{c_{p,n}} \cdot \left(\frac{8.89}{12}\right)^3 = \frac{0.50}{0.4254} \cdot \left(\frac{8.89}{12}\right)^3 \approx 0.478 \text{ pu}.$$

Now, K_1 and K_2 may be calculated in the same way as before, i.e., according to (3.7) and (3.9) respectively, but with new values of $P_{g,pu}$ and v_{wind}. This gives

$$\begin{cases} K_1 = \dfrac{\omega_{pu}}{v_{wind}} = \dfrac{1}{8.89} \approx 0.112486 \\ K_2 = \dfrac{P_{g,pu}}{v_{wind}^3} = \dfrac{0.478}{8.89^3} \approx 0.000680. \end{cases}$$

Applying the new values of K_1 and K_2 to solve the system of equations in (3.10) with $v_{wind,1} = 5.5$ m/s, $v_{wind,2} = 7.0$ m/s and $v_{wind,3} = 8.89$ m/s finally gives the new speed curve coefficients

$$\begin{bmatrix} A_0 \\ A_1 \\ A_2 \end{bmatrix} = \begin{bmatrix} 0.420989 \\ 1.912509 \\ -1.466922 \end{bmatrix}.$$

The new speed reference curve which has been used throughout this thesis is shown in Figure 5.1. In contrast to Figure 3.5, it can be seen that the reference speed is 1.0 pu already from 0.5 pu power and upwards.

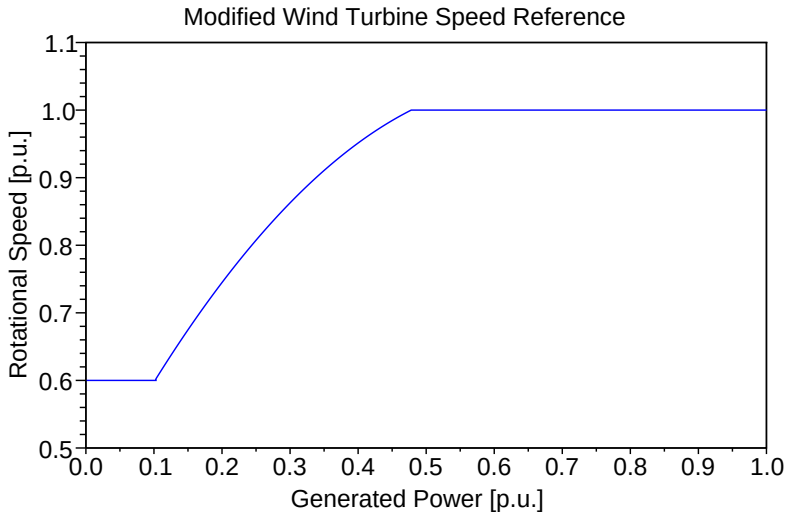

Figure 5.1: Speed reference curve for a wind turbine with a rated wind speed of 12 m/s, using the modified speed controller described in Section 5.1.

5.2 Demonstration of the Modified Speed Controller

To demonstrate the functionality of the modified speed controller, a simulation was done with a wind series ranging from above rated wind, 12 m/s, to below the cut-in wind of 2 m/s. The result of this simulation is shown in Figure 5.2. In the upper part of the graph, the wind speed, the values of c_p and the pitch angle can be seen. It is noted that the speed controller maintains c_p up to a wind of approximately 9 m/s. For the rated wind of 12 m/s, c_p is lower than its maximum

value, namely around 0.42. The pitch angle behaves like expected and mainly pitches the blades for strong winds, i.e., above rated wind. There is also a deflection of the pitch angle at about 370 seconds, when the wind increases from 11 to 12 m/s. Normally, this would not be expected but it is a result of the turbine speed deviating from its reference value due to the wind speed change. This causes an input $\Delta\omega$ to the pitch controller which is large enough to result in a pitching of the blades, cf. Figure 3.6. Nonetheless, in the lower part of the graph, it is seen that the turbine speed follows the reference value in a satisfactory way. It returns to its reference value quickly after having deviated from it during wind speed changes. The produced power is seen to change according to the wind, reaching its rated value for wind speeds of 12 m/s and above. At around 1000 seconds into the simulation, the wind falls to such low values that the produced power will be so low that in turn, the turbine reference speed remains constant at its minimum value. Eventually, the turbine shuts down before 1200 seconds when the wind speed reaches the cut-in wind of 2 m/s. Lastly, comparing these simulation results with the speed reference curve in Figure 5.1, it shows that the turbine does as expected. It reaches nominal operating speed already at approximately 220 seconds when the power generation is around 0.5 pu.

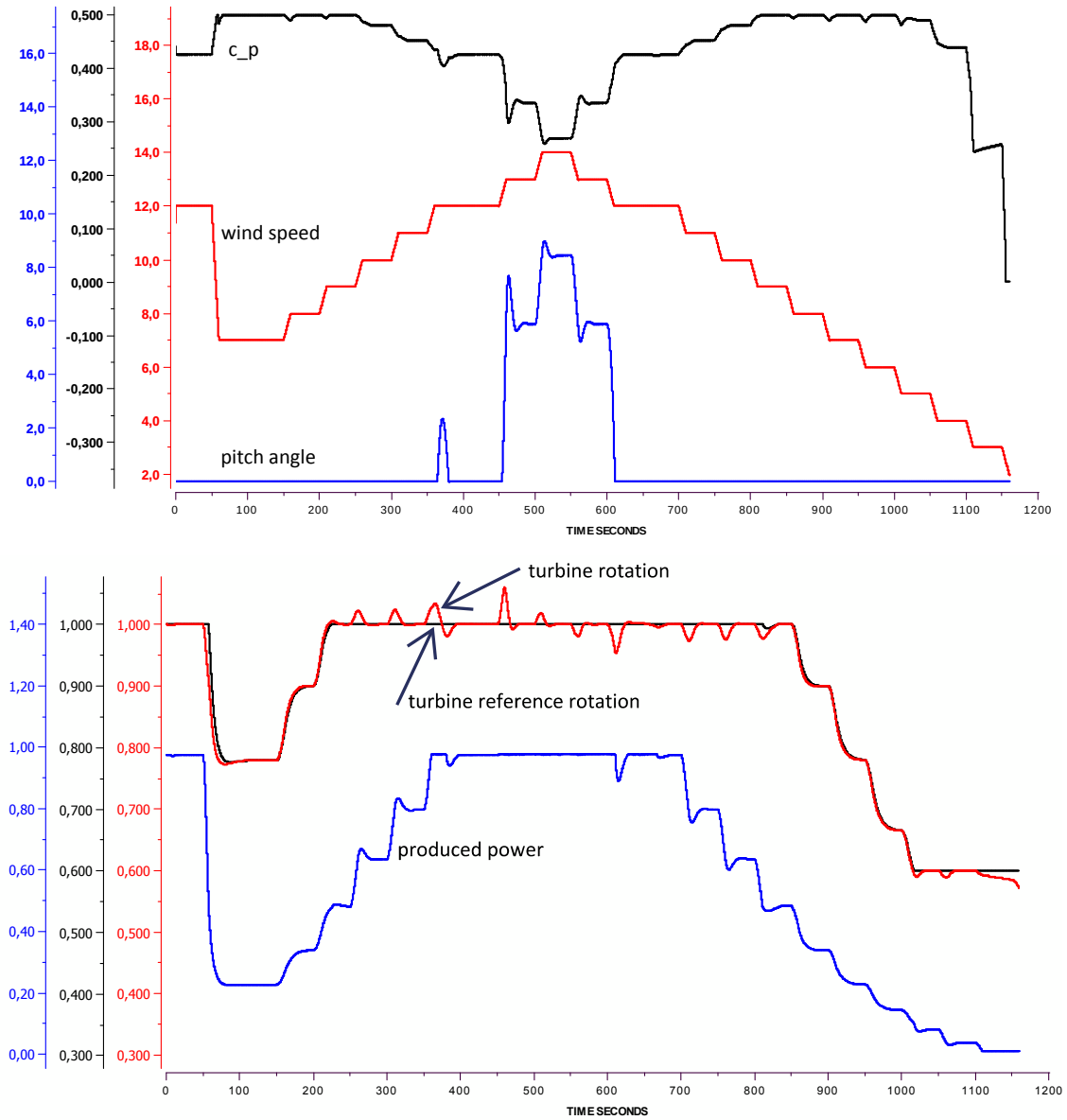

Figure 5.2: Demonstration of the wind turbine model using the modified speed controller. Here the wind turbine runs in an unregulated mode, i.e., it is neither frequency nor power controlled.

Chapter 6

Results and Analysis of Frequency and Active Power Feedback Control

In this chapter, the layout of the simulated power system is first presented. Next, some of the input data to the implemented model is listed to clarify how the simulations have been performed. Following that, the actual simulation results for different deloading levels and turbine control modes, namely frequency regulation (f-reg), active power feedback regulation (P-reg) and combined frequency and power regulation (c-reg), are presented and analysed. A brief investigation of the effect on the frequency of higher wind power penetration is made. The result chapter ends with a study of how the wind turbine performs without regulation of the pitch controller when using the active power feedback control.

6.1 Simulated Power System

The power system used in the simulations is an islanded system with hydro power plants and a wind farm rated at 61.5 MVA or 60 MW. The hydro generators are all modelled as type 1 generators in SIMPOW, cf. Section 3.4, meaning that they are modelled with a field winding, one d-axis damper winding, two q-axis damper windings and including saturation. Adding to that, they are implemented together with PID based governors providing active frequency control, though the droop setting of each production unit is set to 0 %. The system consists of 24 nodes, as shown in Figure 6.1. The main voltage level of the system is 150 kV and all generators are connected through step-up transformers. The power flow calculation, which is run in the SIMPOW module optpow, uses the generator called G1 as the swing bus. The wind power production level is set to 60 MW, assuming at least nominal wind conditions.

The simulations in this chapter are primarily made with a total hydro power capacity of 285 MVA spread over six generators as listed in Table 6.1. Looking at the system load, it sums up to a total of around 203 MW and 99 MVAr. The loads are modelled as simple P and Q loads, non-frequency dependent and without inertia . This configuration gives an installed wind power share of approximately 22 %. The exception from this set-up is found in Section 6.5 where results are presented for a case with 36 % installed wind power. This set-up has been emulated by disconnecting generators G_2 and G_5, giving a total hydro capacity of 169 MVA. Together with the decrease in generating capacity, the load has been decreased according to the initial loading level of generators G_2 and G_5, giving a total load of 143 MW and 70 MVAr.

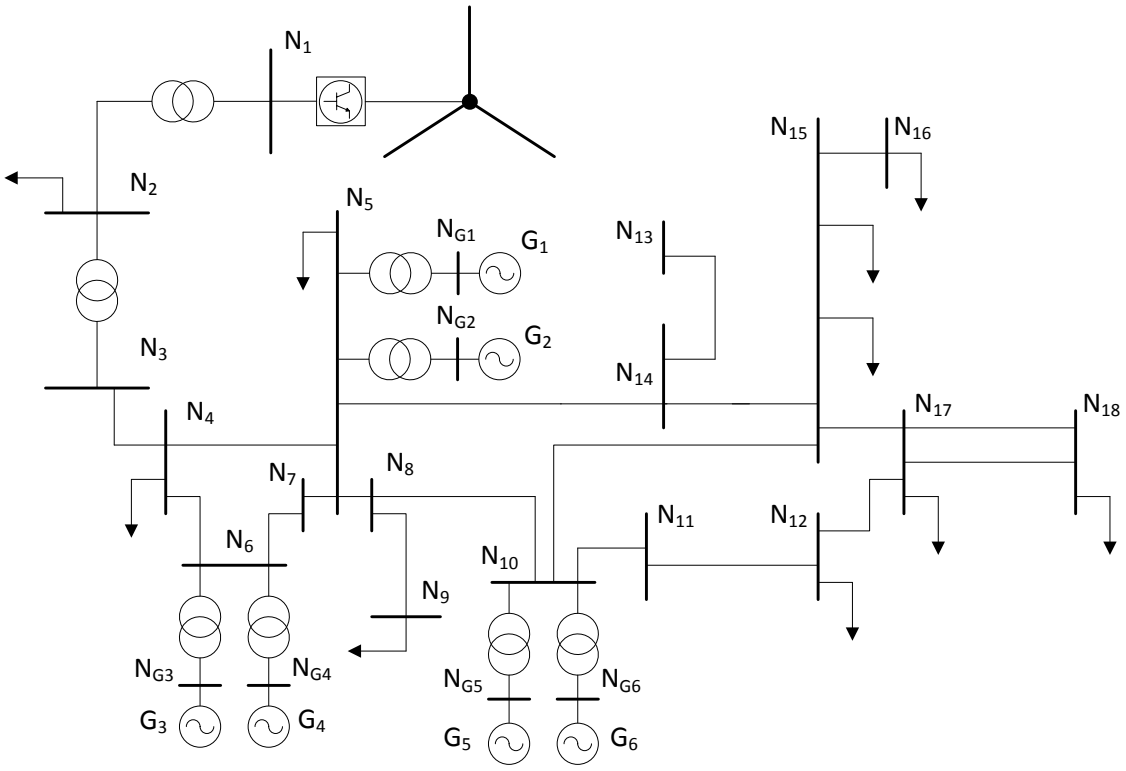

Figure 6.1: Topology of the simulated power system.

Table 6.1: Basic data of the generators in the simulated power system island.

Production node	Rated power [MVA]	Rated voltage [kV]	Inertia constant H [s]
G_1	25	6.6	2
G_2	26	11	2
G_3	27	11	2
G_4	27	11	2
G_5	90	16	3
G_6	90	16	3
Total capacity	285		

6.2 Wind Power Data

The details of the wind power modelling in SIMPOW have previously been described in Chapters 3 and 5. The simulations made in this thesis use an aggregated wind farm with a rated power of 60 MW. The aggregation is done by letting the wind farm consist of 20 3 MW wind turbines and then following the description in Section 3.3. The only variables affected by the aggregation are the nominal power S_n, nominal turbine speed ω_n and blade length R. R_{farm} is calculated by inserting nominal values into (3.9) and finding the radius from the swept area A. $\omega_{n,farm}$ is likewise calculated by using (3.7) with nominal values inserted and then converted to rounds per minute. Finally, another important set of data is the $c_p(\lambda)$ curves. The ones used in this project are taken from [2] and they are plotted in Figure 6.2. In case the pitch angle lies between one of these curves, SIMPOW automatically interpolates an estimated value between the relevant curves [18].

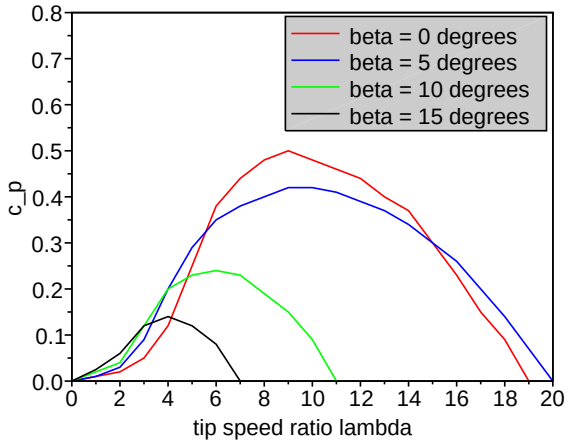

Figure 6.2: $c_p(\lambda)$ curves used in the simulations.

6.3 Comparison of Deloading Levels

First among the results, a comparison between different deloading levels is presented. The purpose of this comparison is to introduce the effect of different pitch angle offsets. Understanding this is important in order to understand the other simulation results. However, the comparison made in this thesis is not complete. It is only made under normal wind fluctuations and not in extreme wind. The previous work done by ÅF in [20] presents a complete study on this specific topic.

The turbine deloading is accomplished by increasing the pitch angle offset β_0. The default value $\beta_0 = -1$ guarantees that the blades will only pitch for wind speeds greater than the nominal wind, i.e., when the speed deviation becomes large enough to overcome the default offset. However, giving β_0 a positive value will result in the blades being pitched with this value at the beginning of each simulation. Depending on the character of the wind series and the state of the surrounding power system, the pitch angle may thereafter increase or decrease. The pitch offset makes the turbine capture less wind and thereby generate less power. This non-optimal wind capture is the energy buffer that makes up the turbine deloading and causes the power curtailment.

To determine suitable deloading levels, a simulation with the unregulated wind power model and the normal wind series was run. This set up constitutes the true Maximum Power Point Tracking case and functions as a reference for all other simulations. The energy of the MPPT with 0° pitch offset was calculated. Subsequent simulations with the unregulated wind turbine were run, but this time with a positive β offset. Comparing the energy yield of each run, the 3.3° pitch offset was determined so that it would yield 95 % energy in normal wind. The 6.0° pitch offset was determined to give 80 % of the energy of the reference case, i.e., the MPPT case without deloading. These β offsets were kept in extreme wind as well, even though the energy yield at $\beta = 6.0^\circ$ turns out to be somewhat higher than 80 %. The legends in the plots state which deloading level that has been utilized, as well as which control concept. The one called “f-reg” is the frequency control method from [20] and the one called “P-reg” is the active power feedback control which has been developed in this thesis. The “P-reg” control is sometimes also called power smoothing control.

6.3.1 Maximum Power Point Tracking

Looking first at the MPPT control scheme and the plots in Figure 6.3 and 6.4, we can see that the frequency has its largest dips at around 190 and 290 seconds of the normal wind variations series, dipping to about 49.6 Hz. Prior to the first of these two events, the frequency has two peaks and before the second dip it has one peak. This may naturally be explained by looking at the normal wind curve plotted in Figure 4.6, which makes the power generation peak at around 180 and 280 seconds in turn causing the frequency peaks. The reason why the frequency drops as drastically as it does after these peaks is that even though the hydro power plants contribute to primary frequency control, they are not fast enough to compensate for the sudden decrease of wind power that occurs when the wind drops.

Concentrating on the different deloading levels, i.e. the different pitch angle offsets, it may be observed that even though no active frequency control is applied in these simulations, the frequency excursions significantly decrease with increased deloading level. This is clearly seen in Figure 6.3 where the frequency result for different deloading levels is shown. With a pitch offset of 6.0°, the minimum frequency stays at around 49.9 Hz. The price of this frequency improvement is, however, that the energy production is reduced to 80 %, as can be seen in the power plot in Figure 6.4. It may also be seen that the effect of a pitch angle offset is the lower initial power level of the wind turbine and reduced power peaks at 160, 180 and 280 seconds.

The main reason for the better frequency result when applying a pitch angle offset is that when $\beta_0 > 0$, the pitch angle is allowed to decrease from its initial value, which in a relative way will increase the generated power. Furthermore, looking back at the block diagram of the pitch controller in Figure 3.6, we can see that an immediate change of the pitch angle must be due to the output of the PI controller, ω_{reg}, being greater than β_0 (if $\beta_0 < 0$), or due to $\omega_{reg} + \beta_0 > 0$ (if $\beta_0 > 0$), neglecting amplitude limiters. If, under such circumstances, $\Delta\omega$ becomes positive, the pitch angle will be raised immediately, dampening any change in the turbine operation. If, on the other hand, $\beta = 0$, ω_{reg} may be negative. Therefore, it is not certain that the pitch angle will increase as soon as $\Delta\omega$ becomes positive. To make β change to positive values, $\Delta\omega$ has to remain positive long enough to increase the output of the integral part to at least $-(\beta_0 + \mathrm{P} \cdot \Delta\omega)$. The conclusion is that with a positive pitch offset, the pitch angle is allowed to respond immediately to the input $\Delta\omega$, causing an overall smoother frequency curve.

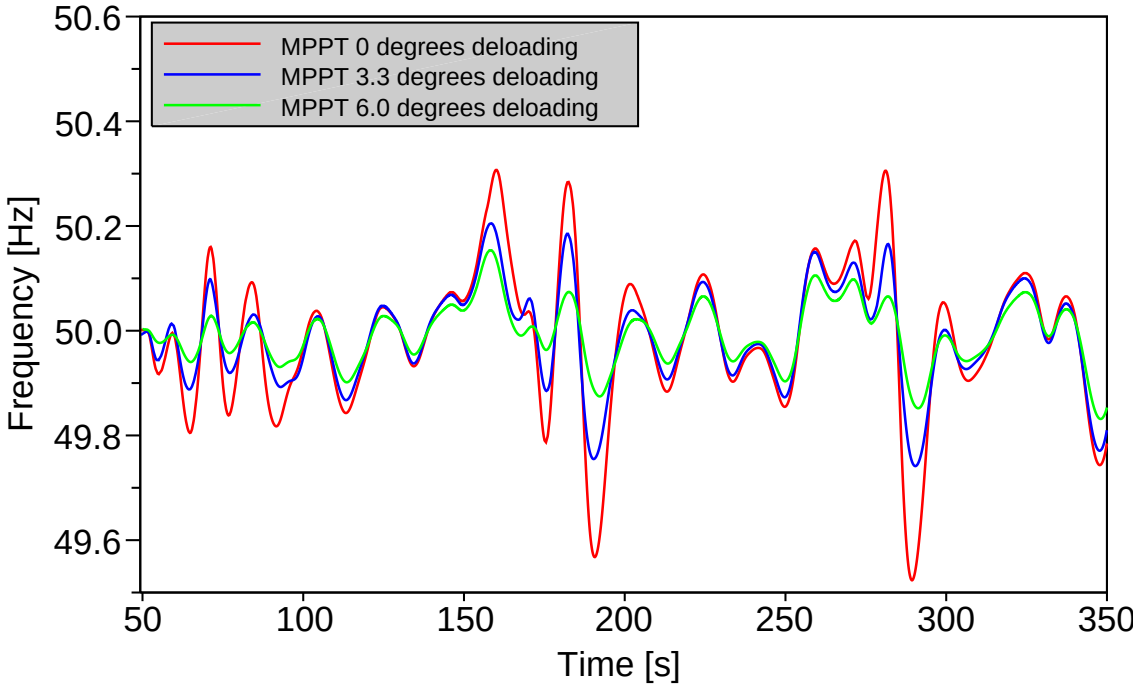

Figure 6.3: Frequency for different deloading levels running MPPT mode, normal wind.

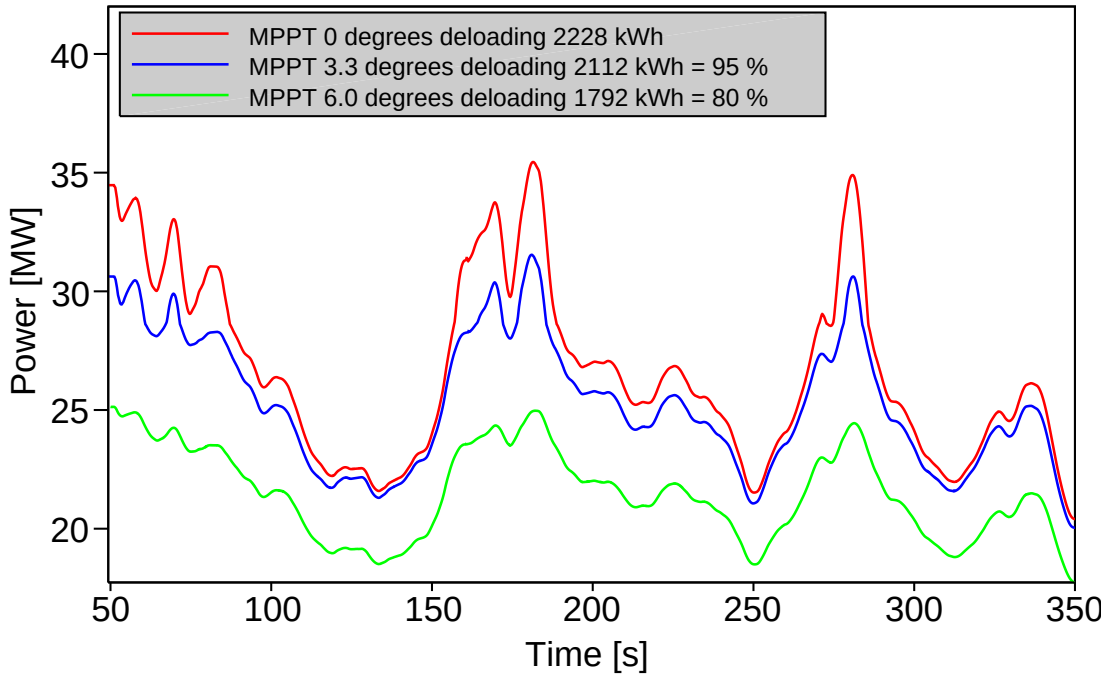

Figure 6.4: Generated power for different deloading levels running MPPT mode, normal wind.

6.3.2 Frequency Control

Having analysed the results for different deloading levels under MPPT operation, next, the outcome when applying the frequency regulation developed by ÅF is shown. The relevant graph for this evaluation is Figure 6.5 showing the frequency of the system. Looking at this plot, it can be seen that the frequency regulation clearly is effective, independent of the turbine deloading level. At 0° deloading the frequency curve is distinctly improved compared to the MPPT case, and at 3.3° and 6.0° deloading the frequency excursions are further reduced. One may specifically look at the time instants of approximately 190 and 290 seconds where the frequency dips are almost erased. This is due to the not so steep power derivate of the generated power when deloading the turbine. When the change in generated power is slower, the hydro generators will be able to better compensate for the decreased wind power generation. In addition, the frequency will be less influenced by a decrease in the wind turbine power when the decrease takes place from a lower, i.e., deloaded, power level. The amount of produced energy is given in Table 6.2. It can be seen that the outcome of applying frequency control to the wind farm is advantageous, since the energy decrease for 0° and 3.3° deloading is only 1 percentage point. In case of 6.0° deloading, the energy production is even equal to the unregulated case (i.e., the MPPT case).

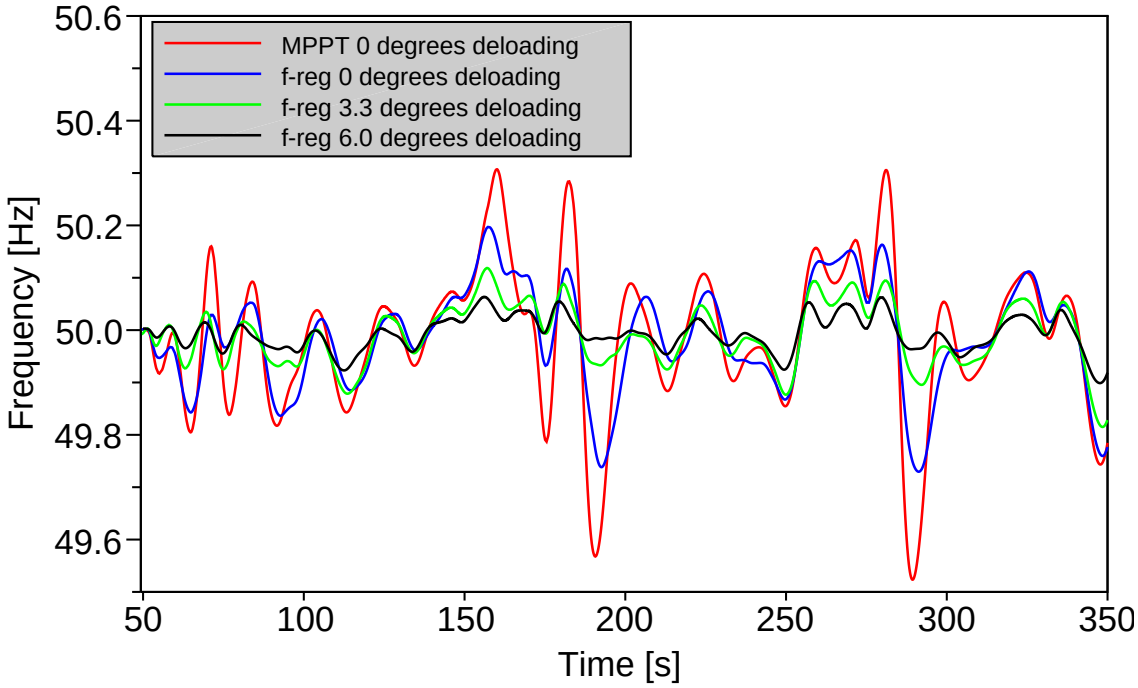

Figure 6.5: Frequency for different deloading levels running f-reg mode, normal wind.

6.3.3 Active Power Feedback Control

The last comparison of deloading levels under normal wind fluctuations is done for the power feedback regulation developed in this thesis. Figure 6.6 shows the frequency curves for this case. Overall, the comparison shows results similar to the frequency control in the Section 6.3.2. From the frequency plot, it is evident that the power feedback control effectively smooths the frequency curve, even without turbine deloading. The dips at around 190 and 290 seconds are effectively mitigated, and at these instances, the power smoothing regulation shows an advantage over the frequency control in the case of no power reserve, cf. Figures 6.5 and 6.6. However, this comes at the price of a slightly lower energy yield, 98 % instead of 99 %. Still, the energy yield of the P-reg method is generally comparable to the f-reg method as well as to the MPPT case, cf. Table 6.2.

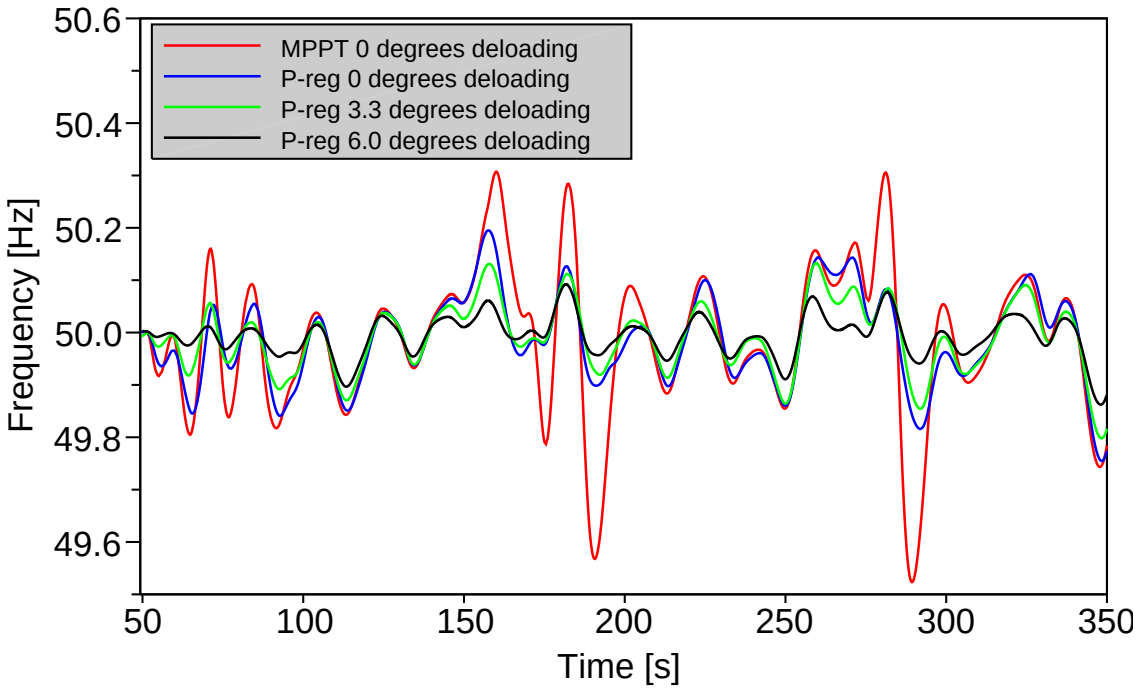

Figure 6.6: Frequency for different deloading levels running P-reg mode, normal wind.

6.3.4 Concluding Remark - Comparison of Deloading Levels

To conclude the comparison of different deloading levels, it can be said that both the frequency control and the active power feedback control clearly improve the system frequency response. The relation between higher deloading, smoother frequency and less energy production remains throughout normal and extreme wind variations. Table 6.2 shows a summary of the different energy yields from Section 6.3. In short, significant frequency stability improvement is possible, though at the drawback of less energy being produced by the wind farm.

Table 6.2: Energy yield for different pitch angle offsets and control methods in normal wind.

Regulation \ Pitch Offset	0°	3.3°	6.0°
MPPT	100 %	95 %	80 %
f-reg	99 %	94 %	80 %
P-reg	98 %	94 %	82 %

6.4 Comparison of Frequency Control and Active Power Feedback Control

The main objective of this section is to compare the active power feedback control developed in this thesis to the frequency control developed by ÅF in [20]. The section is split into two main parts and a concluding remark, of which the first part treats normal wind fluctuations and the second extreme wind fluctuations. To limit the number of cases included, only the case of $\beta_0 = 3.3°$ is treated. Based on the results of Section 6.3, such a deloading is also deemed to be a feasible compromise between frequency stability and loss of energy production. The MPPT case without pitch offset is always plotted as a reference for the results of the different control methods. In this comparison, the combined frequency and power feedback regulation of Section 4.3, called "c-reg", is also included.

6.4.1 Normal Wind Variations

Beginning with the frequency plot, Figure 6.7, the initial observation is that all three applied control methods result in a significantly better frequency stability than the unregulated case. Actually, the differences between the various control methods are relatively small. Nevertheless, two trends may be observed. First, that the active power feedback regulation tends to give the highest frequency peaks and the largest dips. Second, that the combined power and frequency regulation, c-reg, gives a marginally smoother frequency curve than the other control approaches, though this is scarcely significant.

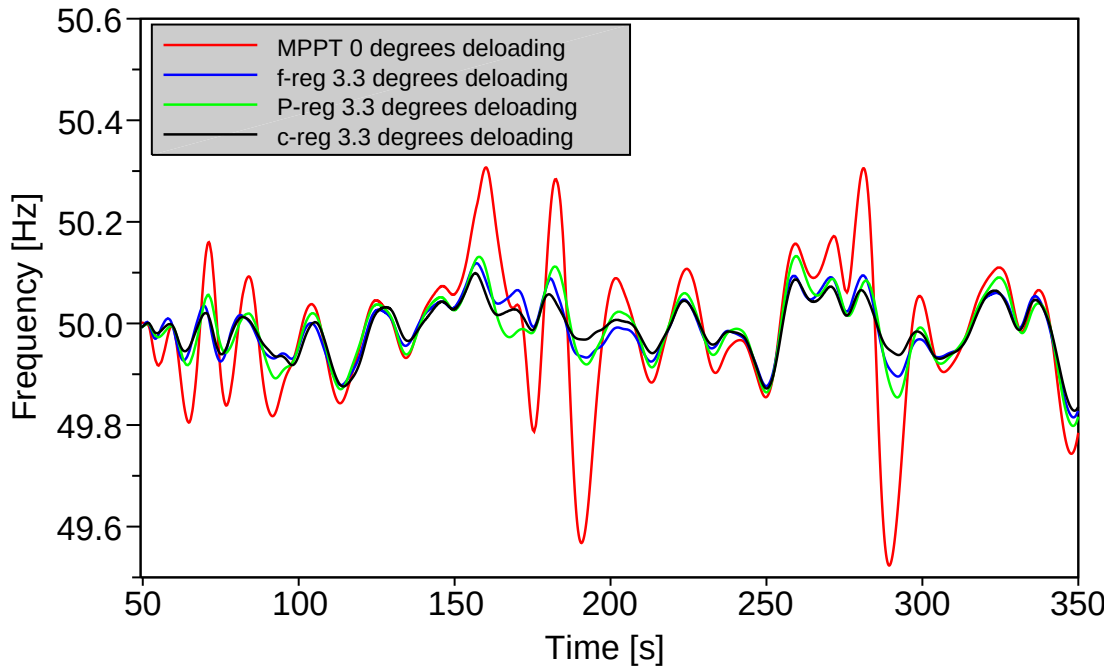

Figure 6.7: Frequency for different regulation methods with $\beta_0 = 3.3°$, normal wind.

Figure 6.8 shows clearly that all of the control methods result in a smoother power curve without the power peaks characterising the non-deloaded MPPT case. All three control methods give equal energy yield, which for the f-reg and the P-reg method of course are the same as in Table 6.2.

Looking at the pitch angle plot in Figure 6.9, the first thing to observe is that in MPPT operation, the pitch angle is down to zero throughout the complete simulation. This is expected, since the default FPCWT model in SIMPOW only should pitch the blades for wind speeds above the

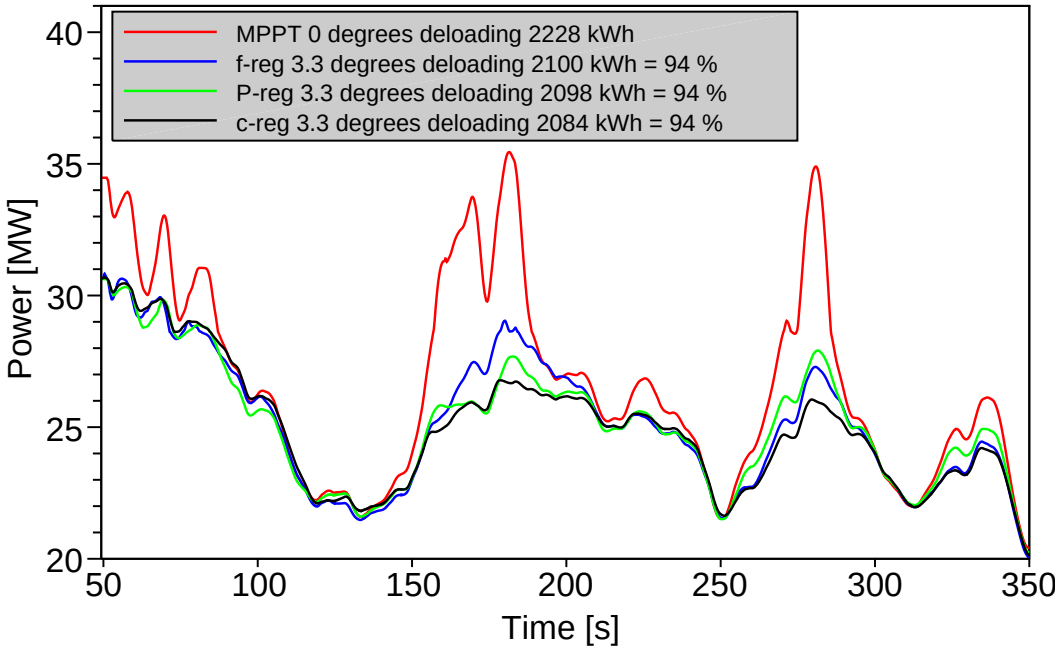

Figure 6.8: Power for different regulation methods with $\beta_0 = 3.3°$, normal wind.

rated wind, which is not the case in the normal wind series. Apart from that, it may be seen that the maximum pitch angle deflection is about 6°. As seen when comparing the pitch angle plot to the power plot in Figure 6.8, the largest pitch angle deflections, roughly between 150 and 180 seconds and between 260 and 390 seconds, correspond timewise to the periods of strong increases in the power curve of the MPPT case. Therefore, it may be concluded that the main reason for the smoother power curves of the regulation methods is the pitch control, which limits the turbine power generation.

The applied control methods will also influence the turbine rotational speed. Simulation results do, however, show that the difference between the MPPT case and the regulated cases is very small.

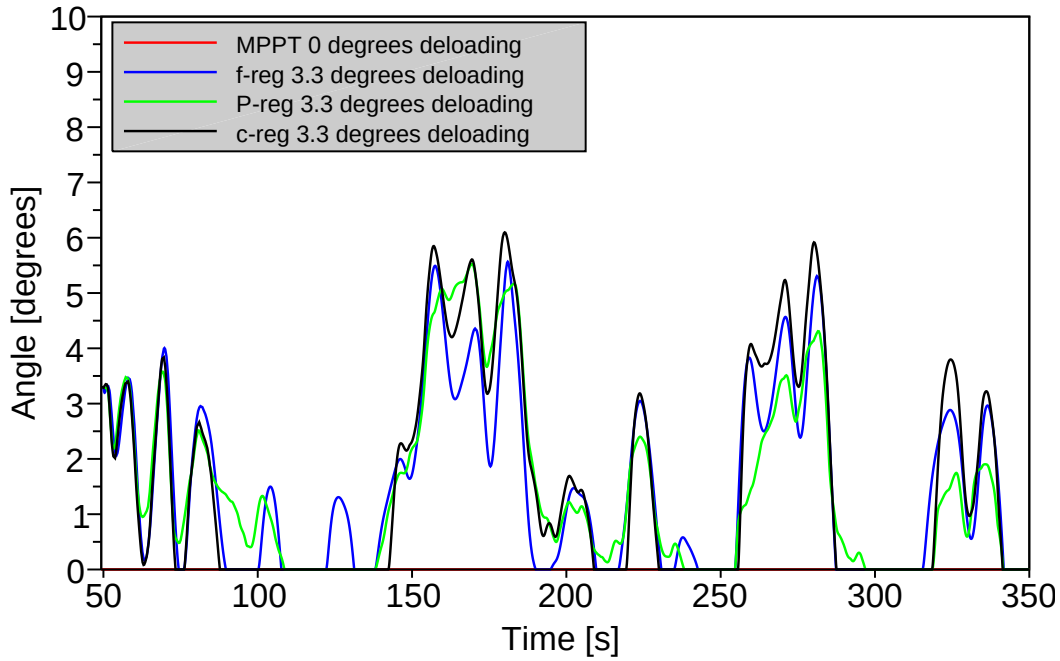

Figure 6.9: Pitch angle for different regulation methods with $\beta_0 = 3.3°$, normal wind.

6.4.2 Extreme Wind Variations

Next, the results under extreme wind conditions, cf. Figure 4.6, are evaluated for the three different regulation methods. First, it is noted that the frequency excursions during extreme wind fluctuations are, as expected, much larger than during normal wind variations. Starting with the frequency plot in Figure 6.10, the severest frequency dips are down below 49.0 Hz. Compared to the normal wind case, this is a severe deterioration, cf. Figure 6.7. It is, however, still within the expected levels in an islanded system with a large share of wind power [4]. The larger frequency fluctuations are partly due to the larger fluctuations of the extreme wind series over the normal wind series, cf. Figure 4.6, but also due to the fact that the extreme wind series lies higher in amplitude than the normal wind series. When the wind series were filtered in [21], this was deliberately done so in order that the extreme wind series should cause as large power and frequency fluctuations as possible. Since it is higher in amplitude and the turbine power is proportional to the cube of the wind speed, any wind speed change occurring at relatively high wind speeds will cause a greater change in the turbine power and the grid frequency, than would the same wind speed change occurring at lower wind speeds.

Looking at the frequency outcome of the different control methods in Figure 6.10, it may be seen that all three control algorithms, like in normal wind (Figure 6.7), clearly improve the frequency curve of the system. Analogously to the normal wind case, the P-reg method gives somewhat higher frequency peaks and greater dips compared to the other methods. The f-reg and c-reg methods are quite comparable, though the f-reg method seems to give slightly lower frequency apexes, and the c-ref method performs slightly better in case of frequency dips.

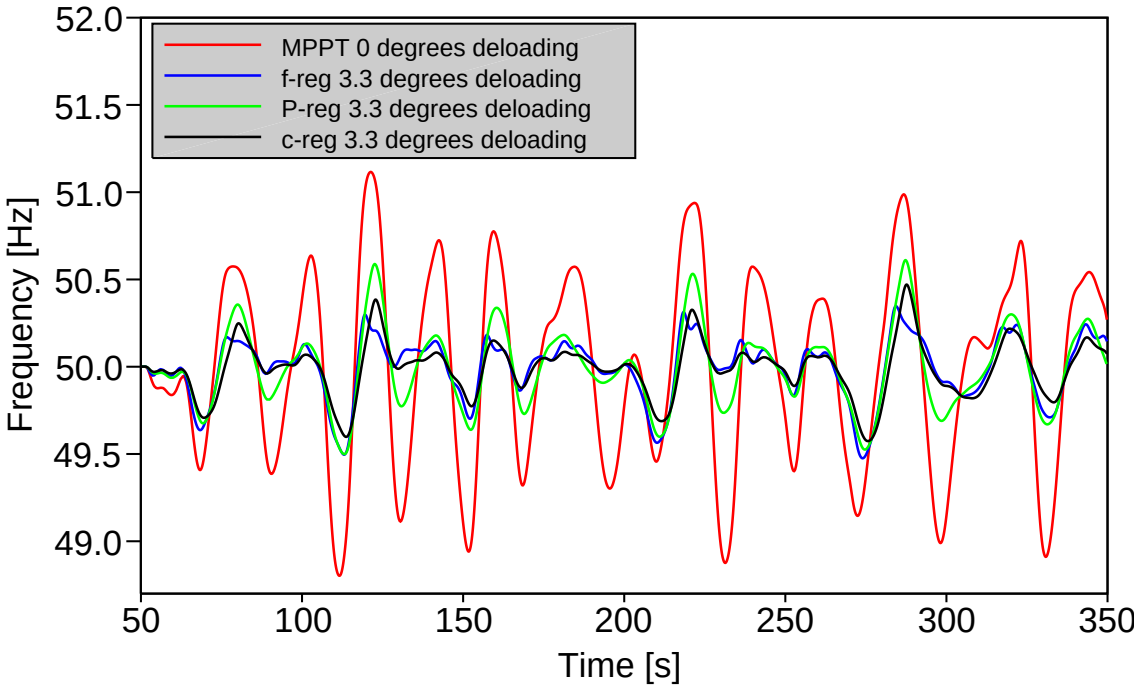

Figure 6.10: Frequency for different regulation methods with $\beta_0 = 3.3°$, extreme wind.

The rapid wind speed changes of the extreme wind series effect the power generation and the pitch angle deflections in a similar manner to the frequency response of the system, i.e., the fluctuations are quicker and larger. The maximum pitch angles will be up to 10°. The active power feedback control gives a slightly higher energy yield of 92 % compared to the other two control methods, cf. Table 6.3. This may, once again, be seen to correspond to the somewhat worse frequency response of the P-reg algorithm.

6.4.3 Concluding Remark - Comparison of Frequency Control and Active Power Feedback Control

To sum up Section 6.4 and the comparison between different regulation methods, it can first be stated that both the frequency control algorithm and the power feedback control algorithm perform well. The results are very similar and it can merely be said that if frequency stability is the major goal, f-reg seems to be slightly better, given a 3.3° pitch angle offset. If power production is the preferred goal, then the P-reg method should be chosen, though its advantage only appears under extreme wind conditions, cf. Table 6.3. The combined power and frequency regulation, the c-reg method, turns out to be very similar to the two other and its use is therefore hard to motivate since it involves a more complex implementation.

Table 6.3: Energy yield for different wind series and control methods using a pitch angle offset of 3.3°.

Regulation \ Wind Series	Normal	Extreme
MPPT	100 %	100 %
f-reg	94 %	90 %
P-reg	94 %	92 %
c-reg	94 %	90 %

6.5 Comparison of Frequency Control and Active Power Feedback Control with Increased Wind Power Share

Following the comparisons made between the different control methods in Section 6.4, this section introduces the issue of increasing the wind power share in a power system and its consequences when applying additional control methods. The simulations here are made with the same aggregated wind farm of 60 MW as previously in this chapter. The amount of hydro power generation and load is however changed to 169 MW generation capacity and 143 MW + j 70 MVAr load, as described in Section 6.1. Making this change to the power system structure gives a situation where the wind farm constitutes approximately 36 % of the installed generating capacity. Due to the decreased load, the loading levels of the remaining hydro generators will match previous simulations. Results are presented for normal wind, using a pitch angle offset of 3.3°.

The only result visualized here is the frequency plot in Figure 6.11. The first observation to be made is the overall larger frequency excursions in this case compared to the system with 22 % installed wind power in Figure 6.7. Comparing these two plots in detail further reveals that shortcoming of the active power feedback control. The inferior performance of the P-ref method when the frequency peaks at around 160 and 180 seconds is worsened when the wind power penetration increases. The result during the frequency dips at around 190 and 290 seconds is similarly aggravated. The conclusion, therefore, is that the active power feedback control works well with a smaller amount of installed wind power and that the advantage of the frequency control method becomes more evident when increasing the wind power penetration. The result of the combined frequency and active power feedback control is almost identical to the frequency control, though partially giving a slightly more levelled frequency curve.

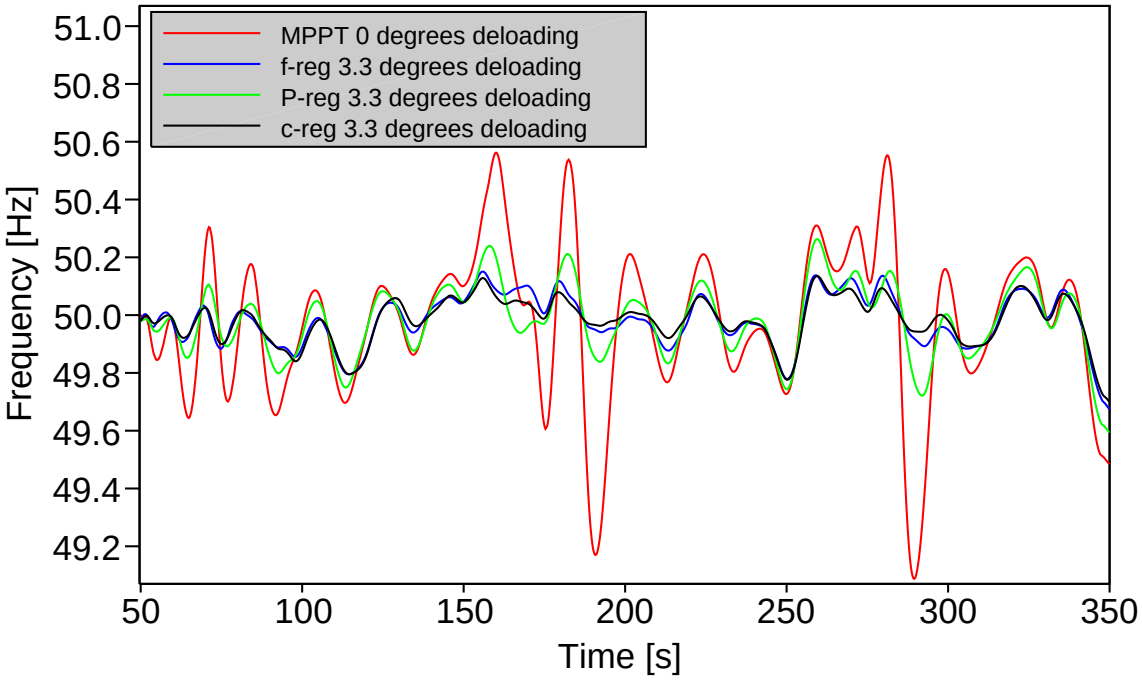

Figure 6.11: Frequency for different regulation methods when increasing the wind power penetration, $\beta_0 = 3.3°$ and normal wind.

6.6 Comparison of Active Power Feedback Regulation with and without Regulated Pitch Control

The final major evaluation that is done is an investigation of the effect of the regulated pitch controller and a pitch angle offset. In all of the previously presented simulation results, the wind turbine is simulated using control algorithms added both to the speed controller and to the pitch controller. The relevant block schemes for the power smoothing regulation method are the ones given in Figure 4.3 and in Figure 4.4. These have so far always been used together. The aim of this section is to evaluate the difference between using both the regulated pitch and the regulated speed controller, as opposed to using the regulated speed controller together with the unregulated pitch controller in Figure 3.6. This comparison is done exclusively for the "P-reg" concept under normal wind conditions. To help identify the strengths and weaknesses of each configuration, the comparison is made with $\beta_0 = 0^\circ$ and $\beta_0 = 3.3^\circ$. Results are shown as frequency, power and pitch angle plots.

6.6.1 0° Deloading

To begin with, the results for 0° deloading are presented. The relevant graphs here are Figures 6.12, 6.13 and 6.14, showing the grid frequency, power generation and pitch angle respectively.

First, the frequency graph is studied, Figure 6.12. According to this plot it is obvious that the frequency curve without regulated pitch controller is worse than with the regulated pitch controller. This is especially clear at the instances of frequency dips at around 190 and 290 seconds, but also in case of frequency apexes at around 160 and 280 seconds.

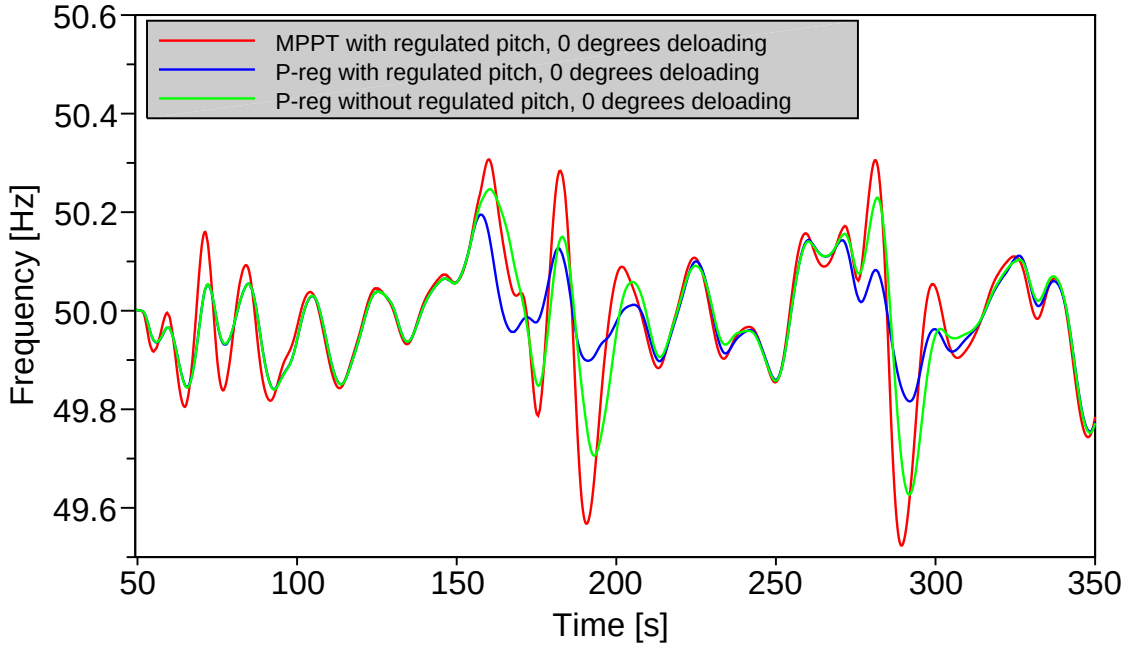

Figure 6.12: Frequency, with and without regulated pitch controller, $\beta_0 = 0^\circ$ and normal wind.

Second, looking at the power plot in Figure 6.13, the effect of the regulated pitch controller is clearly seen, namely that it limits the power generation in case of power peaks. Operating the wind turbine with regulation only on the speed controller is evidently not enough to counteract the large power peaks.

Figure 6.14 shows the pitch angle and gives the explanation to the much better performance of the regulated pitch controller. In case of MPPT operation, the blades are expected to remain

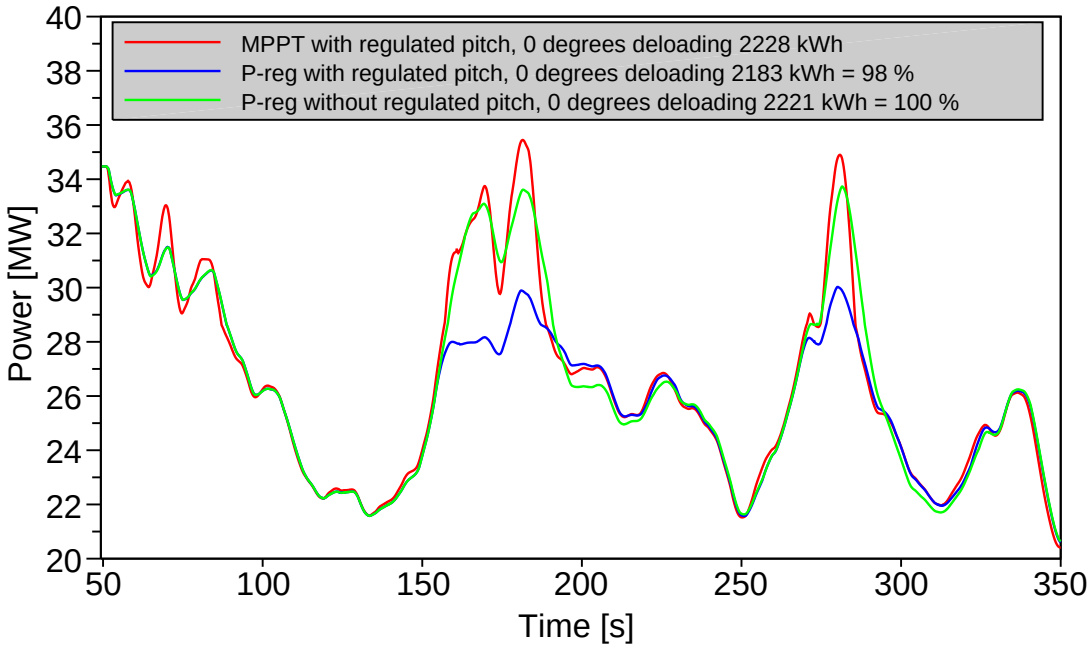

Figure 6.13: Power, with and without regulated pitch controller, $\beta_0 = 0^\circ$ and normal wind.

unpitched, which they do. When there is no active regulation on the pitch controller, it only pitches the blades when the speed deviation $\Delta\omega$ becomes large enough, cf. Figure 3.6. The regulated pitch controller, on the other hand, controls the pitch angle based on its additional input signal, cf. block diagram in Figure 4.4. The result of this is the much more beneficial pitch angle behaviour leading to the better frequency stability. Note that since the turbine is operated without pitch offset, the pitch angle may not decrease from its initial position, wherefore the power generation is only curtailed following an increase in the generated power.

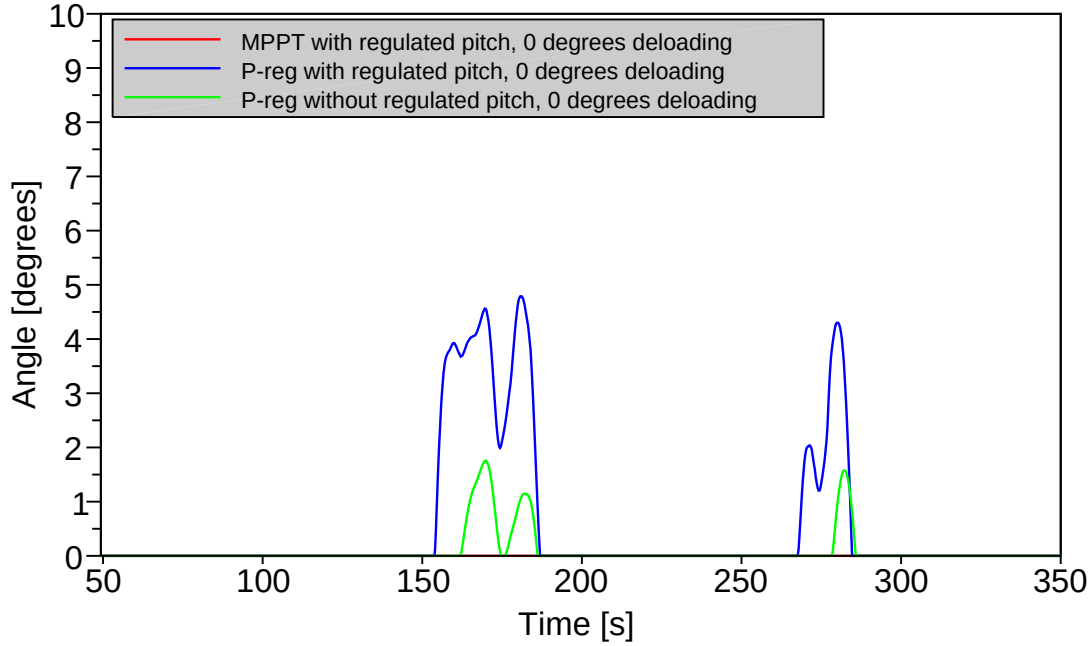

Figure 6.14: Pitch angle, with and without regulated pitch controller, $\beta_0 = 0^\circ$ and normal wind.

6.6.2 3.3° Deloading

In this subsection, the same comparison as in Section 6.6.1 is carried out, though this time with a pitch angle offset of 3.3°.

The frequency plot in Figure 6.15 shows that the frequency curve using the regulated pitch controller is preferable. However, comparing this plot to the one without pitch offset in Figure 6.12, the difference is not as significant, neither in case of frequency dips nor peaks.

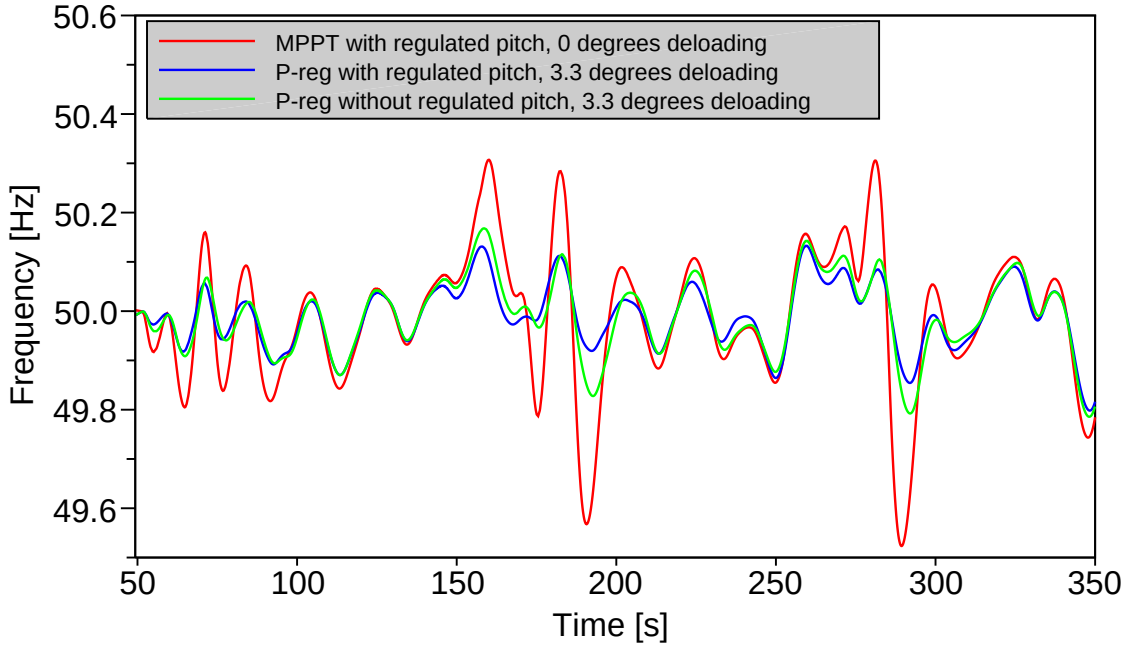

Figure 6.15: Frequency, with and without regulated pitch controller, $\beta_0 = 3.3°$ and normal wind.

The pitch angle offset will make the power generation become smoother both in case of the regulated and the unregulated pitch controller. In both cases, the pitch angle may decrease immediately following a decrease in wind speed, which is not possible when operating the turbine without a pitch offset. The effect of this is the smaller difference between the frequency curves in Figure 6.15 compared to Figure 6.12.

6.6.3 Concluding Remark - Comparison of Active Power Feedback Regulation with and without Regulated Pitch Control

The main conclusion from Section 6.6 and the comparison between the regulated and the unregulated pitch controller is that the regulated pitch controller is of great importance to the frequency stability, especially when operating without pitch offset.

Chapter 7

Application of Full Power Converter Wind Turbines to Power System Black Start

One possible future application of wind power is to use it to black start power systems. In case of a severe contingency leading to a black out, black start capable power plants are needed to bring the electric grid online again. This is done stepwise, beginning with a power plant having black start capabilities, which in the Nordic grid usually is a hydro power plant. Hydro stations are advantageous for this task since they require less auxiliary power than thermal power plants. Once hydro power is available, step-up transformers and transmission lines may be energized in order to transfer power to other bulk production units, restoring the grid step by step. In case of no available hydro power, diesel backup generators may provide cranking power to larger power plants. Possibly, wind turbines could also be used to black start larger production units. If so, turbines with fully rated power converts are preferable since they allow much better grid compliance through the variable speed and the converter control of active and reactive power. These turbines could contribute to normal power generation when the electric grid functions as intended, and in case of a black out they could replace diesel generators and provide the necessary power to black start a larger production unit. Wind turbines are suitable thereto since they require a limited battery backup in order to power yaw motors, blade pitch and other control systems. In order to simulate an actual black starting process, care has to be taken to include in-rush currents of transformers and high voltage lines as well as magnetization of induction motor loads. Such loads are the most common auxiliary power demand of thermal power plants and are used to drive pumps and other mechanical equipment. To secure a safe and stable restoration process, both frequency and voltage have to be controlled and kept within acceptable limits [9], [10].

In the present chapter, a much simplified version of a black start process is simulated. A small grid basically consisting of a wind turbine with a fully rated power converter, transformers, lossless lines, a synchronous generator and a load, see Figure 7.1, is used in these simulations. The intention of the analysis made in this chapter is not to be thorough as in including the electro magnetic transient phenomena of saturation and charging currents mentioned above, but rather to make a first estimation of the feasibility of using wind power plants in this application. A second aspect of this initial study is to see if the frequency based wind turbine control adequately handles these operational challenges.

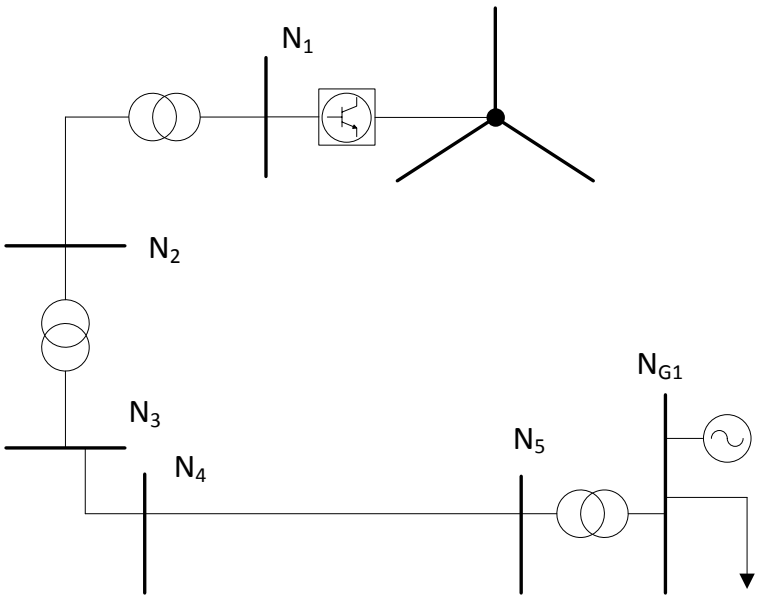

Figure 7.1: System layout of the small power system used for simplified black start studies.

7.1 Description of the Simulated Case

In this chapter, simulation results for a few different cases, with the load in Figure 7.1 being an induction machine, are presented. The simulations are run with the synchronous generator at bus N_{G1} initially being connected. However, 45 seconds into the simulation, the synchronous generator is disconnected and thereafter the wind turbine is the only production source in the grid. The system is run with a single wind turbine of 3 MW and not with a whole wind farm as in Chapter 6.

7.2 Induction Machine Load

The system is simulated using an induction machine as system load. The induction machine has a rated power of 3 MVA, i.e., almost but not exactly equal to the wind turbine rated power, which gives slightly different per unit values of the turbine and the motor. Primarily, simulations are made with a constant wind of 9.6 m/s, making the wind turbine produce 1.83 MW. The induction machine load torque has been matched to this power production in order to render a steady state operating point possible after the disconnection of the synchronous generator. All simulations involving the induction machine load include a load torque change between 100 and 125 second, at which the load torque of the motor is linearly ramped down by 10 % from the initial steady state value. The load torque change implies that the system has to find a new operating point according to the torque speed curve of an induction machine depicted in Figure 7.2.

7.2.1 Without Frequency Control

The first simulated case has been made with an unregulated wind turbine, i.e., it includes neither frequency nor active power feedback control. The wind turbine operates according to the maximum power point tracking principle and the wind is constant. Figures 7.3, 7.4 and 7.5 show the results for the wind turbine and induction machine, as well as the grid voltage and frequency. Looking first at Figure 7.4, it can be seen that the voltage drops to a little more than 0.9 pu when the synchronous generator is disconnected at 45 seconds. This is due to the fact that the synchronous generator reactive power contribution is not substituted by reactive power from the wind turbine,

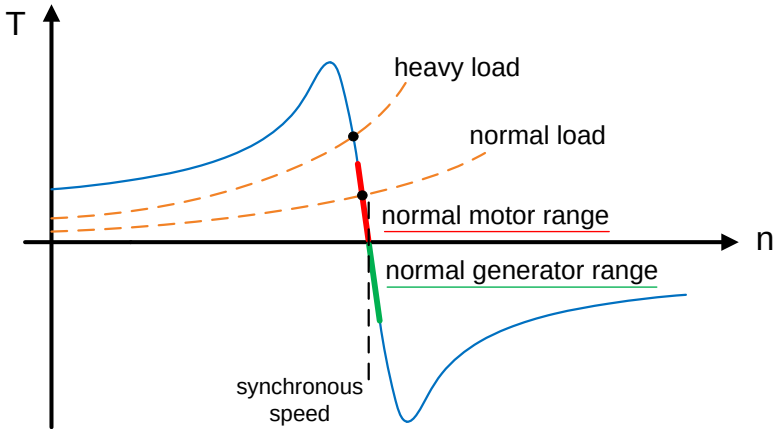

Figure 7.2: Standard torque speed curve of an induction machine.

see Figure 7.5, because the turbine is generally controlled in order to maintain a unity power factor at the wind generator terminals [18]. The spikes at 45 seconds are all due to the tripping of the the synchronous generator. The main thing to observe in these two figures is the change between 100 and 125 seconds, when the motor load torque is decreased by 10 %. Since the power production of the wind turbine is constant due to the constant wind, the driving torque of the induction machine will initially be larger than the braking torque of the load, leading to a speed increase of the motor, in analogy with Equation (2.1). In the simulation, the induction machine operates within the normal motor range of Figure 7.2, meaning that when its speed increases, its torque decreases. Nevertheless, the product of the torque and speed, being power, remains constant and the system finds a new equilibrium when the load torque stabilizes. The motor power is plotted with a negative sign since the power is absorbed. Comparing the speed of the motor in Figure 7.4 to the grid frequency in Figure 7.3, it is noted that both before and after the torque adjustment, the induction machine operates in subsynchronous mode, i.e., as a motor, since the synchronous speed is proportional to the grid frequency. It is clear that the load torque change will cause an undesired increase in the system frequency.

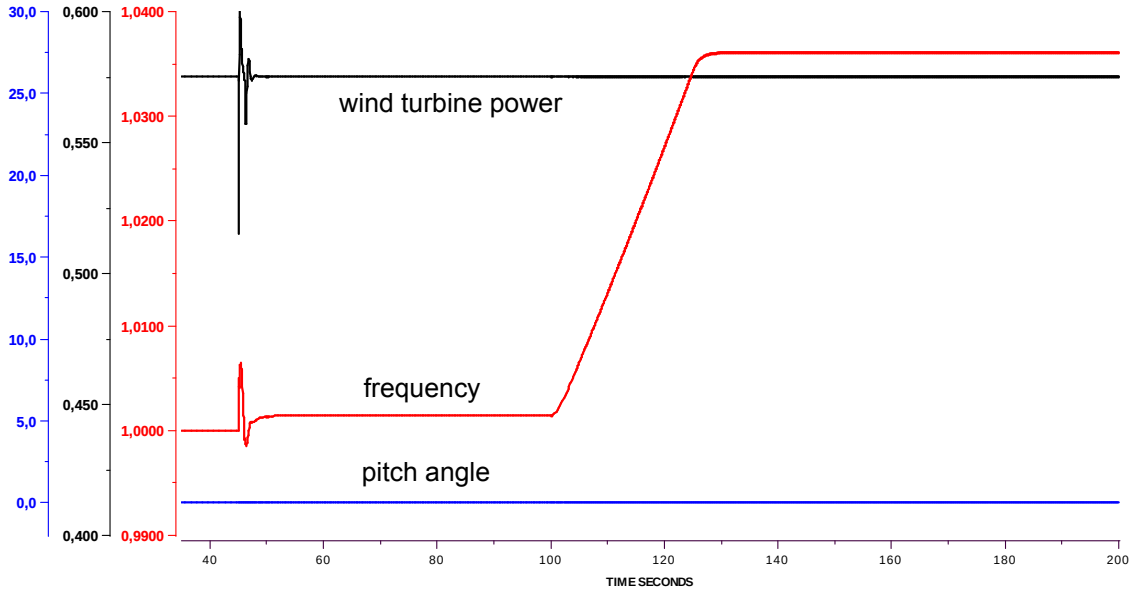

Figure 7.3: Grid frequency, wind turbine power and pitch angle using an unregulated wind turbine and an induction machine load. The synchronous generator is disconnected at 45 seconds.

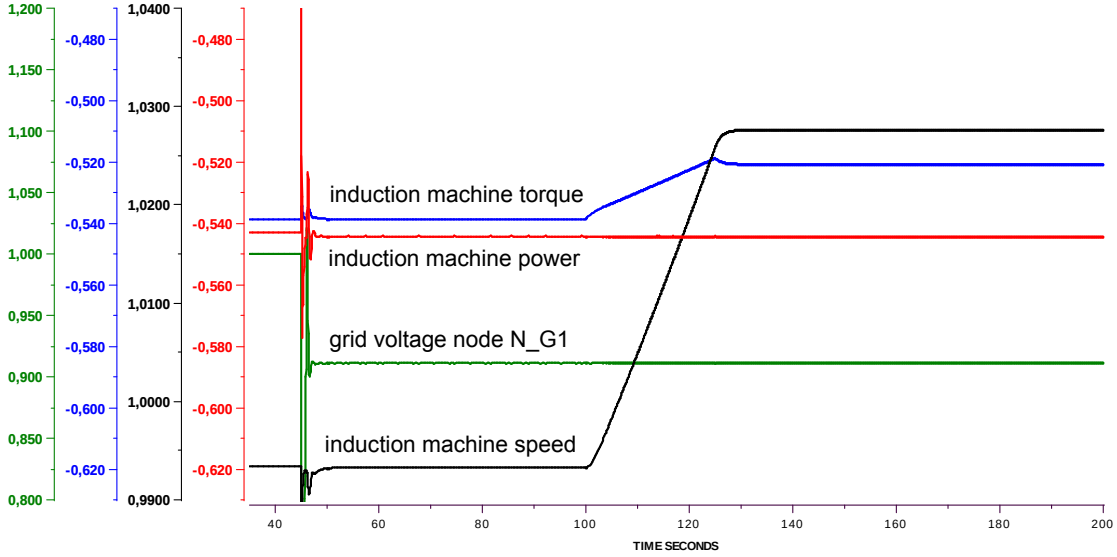

Figure 7.4: Induction machine power, speed and torque, and grid voltage, using an unregulated wind turbine.

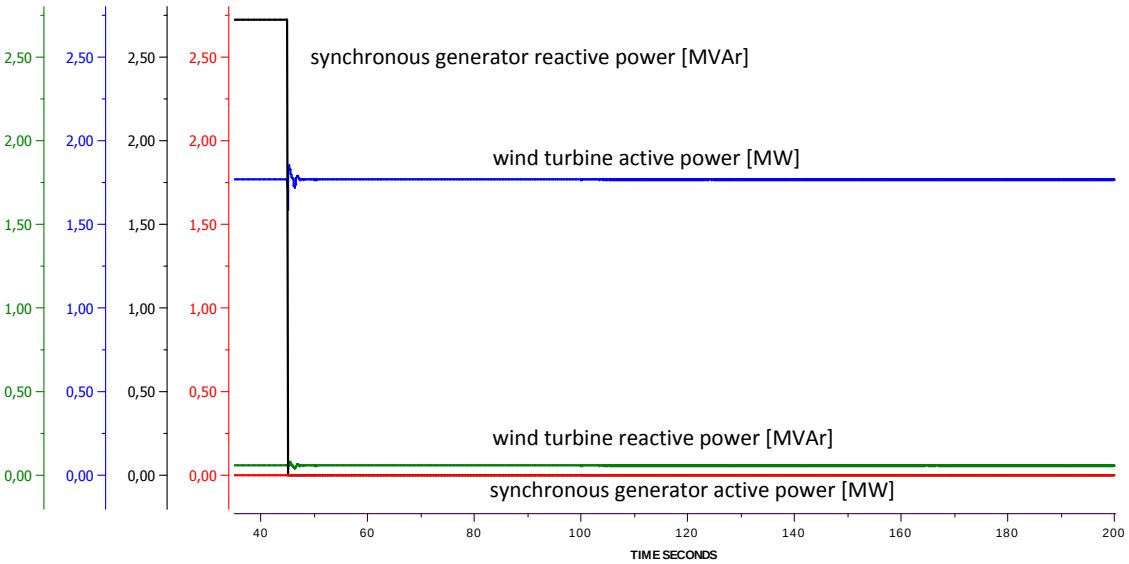

Figure 7.5: Active and reactive power generation of the synchronous generator and the wind turbine, using the an unregulated wind turbine and an induction machine load.

7.2.2 With Frequency Control

The next case to be studied is similar to the previous one, except for the application of frequency control to the wind turbine. The added control is the same used in Chapter 6, there called “f-reg”. Figure 7.6 shows the result for this simulation. The first thing to observe in this plot is the decreased wind turbine power between 100 and 125 seconds. The wind speed is constant, so the power decrease is solely due to the increasing pitch angle. When the induction machine load torque decreases during the said time interval, the speed of the machine increases. The system frequency will likewise increase, due to the lack of synchronous generators controlling the frequency, giving a non-zero input signal to the frequency control system. This will make the pitch angle rise, and thereby the wind turbine will decrease its power generation. Therefore, the speed increase of the induction machine is being limited in comparison to the case without frequency control. As a result of this the power which is absorbed by the motor decreases and the system finds a new steady state operating point after approximately 125 seconds. The advantage of applying frequency control to the wind turbine is readily seen in that the system frequency deviation is less than in the unregulated case, cf. Figure 7.6 to 7.3.

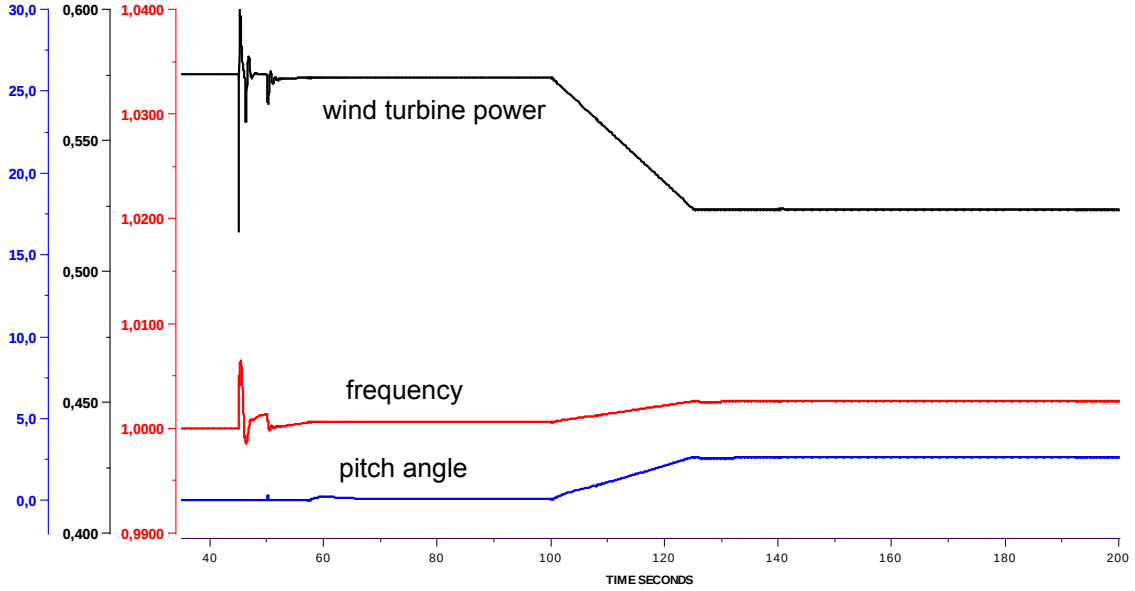

Figure 7.6: Grid frequency, wind turbine power and pitch angle using an induction machine load and applying frequency control to the wind turbine.

7.2.3 Fluctuating Wind Conditions

The last case studied includes normal wind fluctuations. The set-up is basically the same as in Section 7.2.2, but the wind turbine is run with a pitch angle offset of 6.0°. In Chapter 6, 6.0° pitch offset was the largest power reserve investigated, and since frequency stability naturally becomes much more challenging when there are no other production units, the large pitch offset was chosen in this case. In order to achieve a smooth transition when disconnecting the synchronous generator, the initial loading of the induction machine has been adjusted to correspond to the declined power generation of the wind turbine. The wind series used here represents normal wind variations, but it is not filtered according to the aggregated wind farm model.

Looking at Figure 7.7, the effect of the fluctuating wind and the absence of synchronously generating units is obvious. In the figure, the grid frequency can be seen to drop to less than 0.9 pu, which is excessive and would in any normal case trigger under-frequency protection. Large

variations also occur in the induction machine power, torque and speed. An interesting observation is the pitch angle in Figure 7.7, which can be seen to rapidly decrease to zero after the disconnection of the synchronous generator at 45 seconds. Between 85 and 160 seconds into the simulation, the pitch angle is down to zero. It may also be seen that the unmistakable change in the grid frequency commences at around 85 seconds, simultaneous to the blades being completely unpitched. The conclusion therefore, is that an even larger turbine deloading possibly could mitigate the frequency deviation and the overall unstable behaviour of the induction machine. This would of course mean that more wind is being spilled, which, however, is unimportant in the process of system restoration.

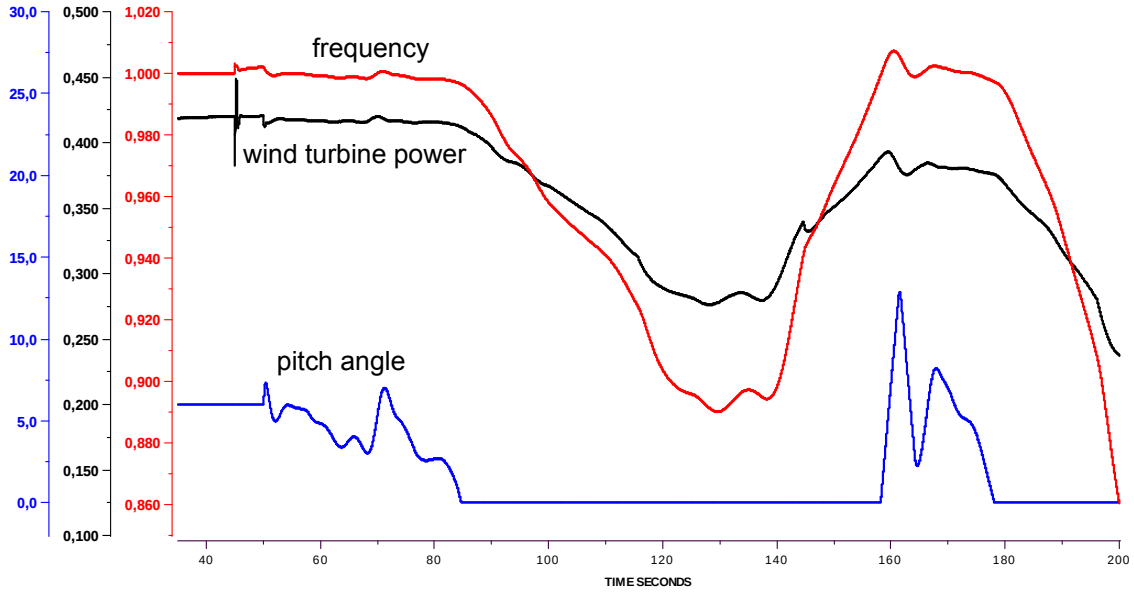

Figure 7.7: Grid frequency, wind turbine power and pitch angle using an induction machine load and applying frequency control to the wind turbine under normal wind fluctuations.

7.2.4 Concluding Remark - Induction Machine Load

The simulation results in this section show the feasibility of applying wind turbine frequency control to very small power systems. Frequency excursions are effectively limited, ensuing from the wind turbine being able to meet the load torque change of the induction machine. However, fluctuating wind conditions put extended demands on the available power reserve of the wind turbine.

Chapter 8

Conclusions

This thesis has shown that there exist good possibilities to control wind turbines in order to increase frequency stability of a power system. An active power feedback control which smooths the power generation has been developed. This control method has been compared to the frequency control developed by ÅF in [20]. According to the results in Chapter 6, they both enhance frequency stability. The frequency control is shown to be superior when the wind power penetration exceeds approximately 25 % of the total system generation capacity, making frequency control the preferable method when increasing the wind power share. It is also shown that a pitch angle offset, or more generally, a power reserve, may contribute to better frequency stability without the implementation of an additional control strategy. Thus, in case of fluctuating wind, a pitch angle offset can in itself achieve a smoother power generation and thereby a smoother grid frequency. Operating a wind turbine with a power reserve will always result in energy – and revenue – being spilled. Requiring wind turbines to participate in frequency control will therefore result in a trade-off between frequency stability and energy production. The exact amount of turbine deloading has to be decided by each wind farm operator in collaboration with the TSO, based on the power system structure, applicable grid codes and possible reimbursement agreements.

The frequency control method has the advantage of being intuitive. Its response to frequency fluctuations is natural and immediate. The active power feedback control, on the other hand, is not as straight forward. It may, for example, happen that the frequency falls below 50 Hz and that the power set point remains below the actual generation level for a certain time. In such a case, the power feedback regulation will drive the turbine production in a direction contrary to what is desired, worsening the frequency deviation. In comparison to the frequency control, the power feedback control is a less intuitive way of controlling the frequency. The main disadvantage is that it does not directly control the frequency but only indirectly through the control of the generated power. Therefore, it becomes more dependent on other generating units to provide true frequency control in order to make the generation follow the load changes.

The active power feedback control was demonstrated in Section 6.6 to be highly dependent on the input of the additional control signal to the pitch controller. Due to the similar appearances of the power and pitch angle graphs for the frequency and the power based control methods in the result chapter, the same conclusion is likely to hold for the frequency based method as well. The results indicate, therefore, that the main component in a successful turbine control is to utilize the pitch control system.

As stated in the beginning of Chapter 7, the investigations made therein are of a much simplified case which in many aspects does not represent a real black start process, lacking first and foremost the component energization. Nonetheless, the simulations made with an induction motor load identifies the need for some kind of frequency control, e.g. when driving motors in the start-up

process of a thermal power plant. The frequency control algorithm was demonstrated to provide such control ability, enabling wind turbines to supply motor loads under these circumstances. It was also shown that when the wind turbine is subjected to varying wind conditions, the frequency stability becomes much more difficult to preserve, requiring a large power reserve through greater turbine deloading.

8.1 Outlook

In this thesis, an aggregated wind farm model has primarily been used. Such an aggregation simplifies the modelling and especially the computational cost of the simulations. As a drawback, it also simplifies the behaviour of a wind farm. To achieve more detailed results, simulations with individual turbines would be preferable to be able to study the frequency response in-depth. Another aspect which has has been left out in this work is that of voltage stability. When dealing with the integration of large wind power shares, voltage stability also has to be considered and studied. How is, for example, the voltage stability margins affected by the implementation of wind power frequency control?

An interesting future work regarding frequency control is to quantify the required deloading levels of wind turbines in order to meet grid code demands. In line with such an investigation, it would be beneficial to investigate the parameter selection of the frequency control algorithm in order to optimize it further. The aim of such an optimization could be to increase the energy yield for a given deloading level, without affecting the frequency stability negatively.

Regarding the issue of applying wind turbines to power system restoration and black start processes, it is undoubtedly necessary to create wind power models valid at the time scale of electromagnetic phenomena. In the process of black starts, energization of transformers and transmission lines put extraordinary requirements on the generating units, making these events a test which wind turbines have to stand to constitute an alternative in black starts.

References

[1] T. Ackermann, Ed., *Wind Power in Power Systems*. Chichester, England: John Wiley & Sons, Ltd, 2005.

[2] H. A. L. Carballido, "Control of a wind turbine equipped with a variable rotor resistance," Master's thesis, Chalmers University of Technology, Göteborg, Sweden, 2009.

[3] R. Carriveau, Ed., *Fundamental and Advanced Topics in Wind Power*. Rijeka, Croatia: InTech, 2011.

[4] *Voltage Characteristics of Electricity Supplied by Public Distribution Networks*, CENELEC European Standard EN 50160:2007, Sep. 2007.

[5] Chowdhury, B.H. and Ma, H.T., "Frequency regulation with wind power plants," in *Power and Energy Society General Meeting - Conversion and Delivery of Electrical Energy in the 21st Century, 2008 IEEE*, july 2008, pp. 1–5.

[6] Conroy, J.F. and Watson, R., "Frequency Response Capability of Full Converter Wind Turbine Generators in Comparison to Conventional Generation," *Power Systems, IEEE Transactions on*, vol. 23, no. 2, pp. 649–656, may 2008.

[7] *Elteknik*, Department of Energy and Environment, Chalmers University of Technology, Gothenburg.

[8] *Network Code for Requirements for Grid Connection applicable to all Generators*, ENTSO-E working draft, Rev. January 24, 2012, Brussels, Belgium.

[9] Feltes, J.W. and Grande-Moran, C., in *Power and Energy Society General Meeting - Conversion and Delivery of Electrical Energy in the 21st Century, 2008 IEEE*.

[10] J. Glover, M. Sarma, and T. Overbye, *Power System Analysis and Design*, 4th ed. Stamford, USA: CENGAGE Learning, 2008.

[11] K. Kleinekorte, "Grundlagen der Systemführung im Transportnetz," lecture notes, RWTH Aachen University, Germany, 2010.

[12] P. Kundur, *Power System Stability and Control*, N. J. Balu and M. G. Lauby, Eds. New York, USA: McGraw-Hill, 1994.

[13] E. Loukarakis, I. Margaris, and P. Moutis, "Frequency Control Support and Participation Methods Provided by Wind Generation," in *Electrical Power Energy Conference (EPEC), 2009 IEEE*, oct. 2009, pp. 1–6.

[14] J. Machowski, J. W. Bialek, and J. R. Bumby, *Power System Dynamics Stability and Control*, 2nd ed. Chichester, United Kingdom: John Wiley & Sons, Ltd, 2008.

[15] Margaris, I.D. and Papathanassiou, S.A. and Hatziargyriou, N.D. and Hansen, A.D. and Sorensen, P., "Frequency Control in Autonomous Power Systems With High Wind Power Penetration," *Sustainable Energy, IEEE Transactions on*, vol. 3, no. 2, pp. 189–199, april 2012.

[16] *Nordic Grid Code 2007*, Nordel Std., Rev. January 15 2007.

[17] SIMPOW®, *Power system simulation software*, Manitoba HVDC Research Centre, 211 Commerce Drive, Winnipeg, Manitoba, Canada.

[18] *SIMPOW® USER MANUAL 11.0*, STRI, 2010.

[19] Tarnowski, G.C. and Kjær, P.C. and Dalsgaard, S. and Nyborg, A., "Regulation and Frequency Response Service Capability of Modern Wind Power Plants," in *Power and Energy Society General Meeting, 2010 IEEE*, july 2010, pp. 1–8.

[20] M. Wang-Hansen, R. Josefsson, and H. Mehmedovic, "Frequency Controlling Wind Power - Modeling of Control Strategies," ÅF Industry, 2012.

[21] M. Wang-Hansen and H. Mehmedovic, "Svenska Kraftnät Studie av vindkraft som produktionskälla i ö-drift," ÅF Industry, 2010.

[22] "World Wind Energy Report 2010," World Wind Energy Association, 2011, accessed 2012-05-29. [Online]. Available: http://www.wwindea.org/home/images/stories/pdfs/worldwindenergyreport2010_s.pdf

[23] Y. zhang Sun, Z. sui Zhang, G. jie Li, and J. Lin, "Review on Frequency Control of Power Systems with Wind Power Penetration," in *Power System Technology (POWERCON), 2010 International Conference on*, oct. 2010, pp. 1–8.